THE JOURNAL OF BIOLOGICAL CHEMISTRY VOL. 280, NO. 37, pp. 32379–32388, September 16, 2005


# T-oligo Treatment Decreases Constitutive and UVB-induced COX-2 Levels through p53- and NFκB-dependent Repression of the COX-2 Promoter*[S]

Received for publication, March 24, 2005, and in revised form, July 14, 2005 Published, JBC Papers in Press, July 26, 2005, DOI 10.1074/jbc.M503245200

Vaneeta Marwaha[‡1], Ya-Hui Chen[‡1,2], Elizabeth Helms[‡], Simin Arad[‡], Hiroyasu Inoue[§], Evelyn Bord[¶], Raj Kishore[¶], Raffi Der Sarkissian[‖], Barbara A. Gilchrest[‡3], and David A. Goukassian[‡4]

*From the [‡]Departments of Dermatology and [‖]Division of Facial Plastic and Reconstructive Surgery, Boston University School of Medicine, Boston, Massachusetts 02118, [§]Nara Women's University, Nara 630-8506, Japan and [¶]Division of Cardiovascular Research, St. Elizabeth's Medical Center, Boston, Massachusetts 02135*

Chronically irradiated murine skin and UV light-induced squamous cell carcinomas overexpress the inducible isoform of cyclooxygenase (COX-2), and COX-2 inhibition reduces photocarcinogenesis in mice. We have reported previously that DNA oligonucleotides substantially homologous to the telomere 3′-overhang (T-oligos) induce DNA repair capacity and multiple other cancer prevention responses, in part through up-regulation and activation of p53. To determine whether T-oligos affect COX-2 expression, human newborn keratinocytes and fibroblasts were pretreated with T-oligos or diluent alone for 24 h, UV-irradiated, and processed for Western blotting. In both cell types, T-oligos transcriptionally down-regulated base-line and UV light-induced COX-2 expression, coincident with p53 activation. In fibroblasts with wild type versus dominant negative p53 ($p53^{WT}$ versus $p53^{DN}$), T-oligos decreased constitutive expression of a COX-2 reporter plasmid by >50%. We then examined NFκB, a known positive regulator of COX-2 transcription. In $p53^{WT}$ but not in $p53^{DN}$ fibroblasts and in human keratinocytes, T-oligos decreased readout of an NFκB promoter-driven reporter plasmid and decreased NFκB binding to DNA. After T-oligo treatment and subsequent UV irradiation, binding of the transcriptional co-activator protein p300 to NFκB was decreased, whereas binding of p300 to p53 was increased. Human skin explants provided with T-oligos had markedly decreased COX-2 immunostaining both at base-line and post-UV light, coincident with increased p53 immunostaining. We conclude that T-oligos transcriptionally down-regulate COX-2 expression in human skin via activation and up-regulation of p53, at least in part by inhibiting NFκB transcriptional activation. Decreased COX-2 expression may contribute to the observed ability of T-oligos to reduce photocarcinogenesis.

Nonmelanoma skin cancer accounts for well over 1 million cases of human malignancy annually in the United States, and the incidence continues to rise (1–3). The major initiator and promoter of skin cancer is UVB radiation (4, 5). Among the contributing effects of UVB radiation on skin are the formation of cyclobutane-pyrimidine dimers and pyrimidine (6-4) photoproducts (6, 7), which lead to mutations in key regulatory genes (8), epidermal hyperplasia (9, 10) allowing for expansion of mutated clones (11), immunosuppression (12, 13), and inflammation (14, 15).

One way inflammation in particular is thought to affect carcinogenesis is by promoting epidermal hyperplasia and proliferation through production of cytokines and various second messengers such as prostaglandin $E_2$ (16). The major enzyme responsible for the UVB-induced prostaglandin synthesis is cyclooxygenase-2 (COX-2),[5] the inducible isoform of the cyclooxygenase enzyme (17) that carries out the rate-limiting step of prostaglandin and thromboxane production (18–20). COX-2 has been shown to be overexpressed in numerous human malignancies, including colon, lung, and breast cancers (21–24). In relation to skin cancer, UVB irradiation increases both mRNA and protein levels of COX-2 in human keratinocytes (25). Recent studies have shown increased COX-2 expression in human skin in response to acute UVB exposure as well as increased COX-2 expression in human and murine tumors that were induced by chronic UVB exposure (26, 27). Furthermore, specific inhibitors of Cox-2 such as celecoxib have been shown not only to decrease tumorigenesis and increase tumor latency in hairless mice models (28) but also to decrease tumor growth in hairless mice with pre-existing UVB-induced tumors (29). In addition, Cox-2-overexpressing transgenic mice have shown dramatic increase in predisposition to tumor development in tumor promotion studies (30).

Given the evidence implicating COX-2 in tumorigenesis and tumor maintenance, methods to decrease COX-2 levels in response to UVB irradiation are currently being investigated as a promising means of cancer prevention. Known inhibitors of COX-2 include estrogens, antioxidants, and p53 (31–33). The presence of active p53 in particular has been shown to decrease both the mRNA and protein levels of Cox-2 in mouse embryo fibroblasts (33). In a study of head and neck squamous cell carcinomas (SCCs), tumors with mutated p53 showed higher COX-2 protein levels than tumors expressing wild type (WT) p53 (34). Evidence thus suggests that activating p53 and thereby reducing COX-2 expression in the absence of DNA damage might decrease photocarcinogenesis and inhibit growth of established tumors.

In mammalian cells, telomeres are tandem repeats of a short DNA sequence, 5′-TTAGGG-′ and its complement that cap chromosome

* This work was supported in part by National Institutes of Health Grant RO-1 CA105156-01 and by the Herzog Foundation. The costs of publication of this article were defrayed in part by the payment of page charges. This article must therefore be hereby marked "*advertisement*" in accordance with 18 U.S.C. Section 1734 solely to indicate this fact.

[S] The on-line version of this article (available at http://www.jbc.org) contains Figs. S1–S7.

[1] Both authors contributed equally to this work.

[2] Supported by the Veterans General Hospital, Kaohsiung, Taiwan. Present address: Dept. of Dermatology, Veterans General Hospital, Kaohsiung, Taiwan.

[3] To whom correspondence may be addressed: Dept. of Dermatology, Boston University School of Medicine, 609 Albany St., Boston, MA 02118. Tel.: 617-638-5541; Fax: 617-638-5515; E-mail: bgilchre@bu.edu.

[4] To whom correspondence may be addressed: Dept. of Dermatology, Boston University School of Medicine, 609 Albany St., Boston, MA 02118, Tel.: 617-638-5541; Fax: 617-638-5515; E-mail: dgoukass@bu.edu.

[5] The abbreviations used are: COX-2, cyclooxygenase-2; pTT, thymidine dinucleotide; WT, wild type; DN, dominant negative; SCC, squamous cell carcinoma; T-oligos, telomere homolog oligonucleotide (repeats of TTAGGG); EMSAs, electrophoretic mobility shift assays; TBPs, TATA-binding proteins; ATM, ataxia telangiectasia mutated.

ends and form a large loop structure (35). The loop is held closed by an ~100–400-base single-stranded 3′-overhang that inserts into the proximal double-stranded telomere and is secured by binding proteins, particularly telomere repeat binding factor (TRF2) (36). Disruption of this loop structure by sequestration of the binding protein with a dominant negative construct ($TRF2^{DN}$) leads to exposure of the 3′-overhang sequence (repeats of TTAGGG), digestion of the overhang, and signaling through ATM and p53 that induces DNA damage responses (37). We have found that providing cultured cells with DNA oligonucleotides substantially homologous to the telomere sequence, which we term T-oligos, mimics telomere loop disruption, leading to ATM/p53 signaling (38) and the DNA damage-like responses of senescence (39) or apoptosis (40) but apparently without disruption of the loop or other effects on genomic DNA (40). Because these 2–11-base T-oligos concentrate rapidly in the nucleus (40, 41), we hypothesize that T-oligos are interpreted by the cell as indicating telomere loop disruption, specifically exposure of the otherwise concealed 3′-overhang sequence (38–40), and hence initiate signaling for DNA damage-like responses without antecedent DNA damage.

T-oligos with 100% telomere homology, delivered at a sufficiently high dose, elicit predominantly "end point" cancer protective responses such as apoptosis or proliferative senescence that remove cells, particularly malignant cells, from the proliferative pool (40, 42, 43). However, it is also possible to provide cells with a less than maximal DNA damage signal by reducing the T-oligo dose and/or employing a shorter or less telomere-homologous oligonucleotide. Under these circumstances, it is possible to observe transient reversible cell cycle arrest (44), increased melanogenesis in pigment cells and intact skin (44–46), release of immunomodulatory cytokines from keratinocytes associated with abrogation of allergic contact sensitization or elicitation in intact skin (47, 48), enhanced rate and accuracy of DNA repair both *in vitro* and *in vivo* (49–51), and decreased mutation rate and tumor development *in vivo* (51). Moreover, malignant cells appear to undergo apoptosis or senescence more readily in response to a given T-oligo at a given dose than do their normal nontransformed cellular counterparts (42, 43).

In the present study, we show that treatment with either of two oligonucleotides with partial telomere homology decreases constitutive and UVB-induced COX-2 levels in cultured human fibroblasts, human skin explants, and intact murine skin. These responses are shown to occur at least in part through up-regulation and activation of p53, leading to transcriptional repression of COX-2 promoter activity. We propose that in addition to the previously reported protective DNA damage responses, treatment with T-oligos may also decrease the cutaneous inflammatory response through inhibition of COX-2 expression, a possible additional means of reducing photocarcinogenesis.

## EXPERIMENTAL PROCEDURES

*Cell Culture*—Primary human neonatal fibroblast and keratinocytes cultures were established as described (49, 50). Cells were incubated at 37 °C in 5% $CO_2$. Cell lines permanently (retroviral transfection) expressing WT p53 (R2FWT) or dominant negative p53 (R2FDD) (52–54) were the generous gift from Dr. Jim Rheinwald (Department of Dermatology, Harvard Skin Disease Research Center, Harvard Medical School, Boston) and were maintained in R2F medium containing 42.5% Dulbecco's modified Eagle's medium, 42.5% F-12, 15% calf serum, and 0.1% epidermal growth factor at 37 °C in 5% $CO_2$.

*Oligonucleotides*—Previous experiments have shown that 100 μM of thymidine dinucleotide (pTT), representing one-third of the telomere repeat, and 40 μM of pGAGTATGAG (p9-mer), a 55% homologous sequence, are roughly bioequivalent concentrations for the elicitation of UV mimetic responses (49, 50, 55, 56), including p53 up-regulation and activation. Oligonucleotides (pTT and p9-mer) were synthesized with phosphodiester linkage by Midland Certified Reagent (Midland, TX) and diluted in $H_2O$ to form a 2 mM stock. This stock solution was then diluted in the appropriate culture medium to 100 or 40 μM, respectively, and added to culture dishes for use in experiments. Cells and skin explants were provided T-oligos only once at time 0 and then harvested at intervals, according to the design of the specific experiment. All experiments were conducted using both pTT and p9-mer and gave identical results with either T-oligo.

*UVB Irradiation*—After 48 h of incubation in medium containing pTT, p9-mer, or diluent alone, cells or skin explants were placed in phosphate-buffered saline and irradiated through the plastic culture dish cover by using a solar simulator (Spectral Energy Corp., Westwood, NJ). The 1-kilowatt xenon arc lamp (XMN-1000-21; Optical Radiation Corp., Azuza, CA) irradiance was adjusted to $5 \times 10^{-5}$ watts/cm$^2$, and dishes were exposed to 15 mJ/cm$^2$ as measured with a research radiometer fitted with a UV light probe at 285 ± 5 nm (model IL1700 A; International Light, Newburyport, MA) (56, 57), a protocol that exposes cells to a spectrum of light resembling terrestrial sunlight (58). Sham-irradiated cultures were handled identically, except that they were shielded with aluminum foil during irradiation. After irradiation, cells were given fresh medium lacking T-oligos.

*Western Blot Analysis*—Total cellular proteins were collected as described previously (46). Concentrations were determined by the Bio-Rad method, and 50 μg of protein were run in each lane on a 10% denaturing SDS-polyacrylamide gel. Proteins were then transferred to a nitrocellulose membrane. Antibody reactions were performed with the following antibodies: phospho-$p53^{Ser15}$ (Cell Signaling Technology, Beverly, MA), p53 DO-1, COX-2, NFκB/p65, and actin (all from Santa Cruz Biotechnology, Santa Cruz, CA). Western blot analysis was then performed as described (46).

*Electrophoretic Mobility Shift Assays*—Electrophoretic mobility shift assays (EMSAs) using consensus p53 and NFκB oligonucleotides (Santa Cruz Biotechnology) and 5 μg of nuclear protein from variously treated cells were carried out as described previously (59). Reactions were electrophoresed on 5% nondenaturing polyacrylamide gels, dried, and processed for autoradiography. For competition experiments, 50–100-fold excess of unlabeled DNA were added to the reaction 20 min before the addition of radiolabeled probe.

*Transfection Studies*—Constructs containing the full-length phPES2(−1432/+59) human Cox-2 promoter, a deletion construct of phPES2(−327/+59), and an NFκB binding region site-specific mutant of phPES2(−327/+59) attached to a luciferase reporter (60, 61) or an NFκB reporter plasmid (Promega Corp., Madison, WI) were employed. The pGL2 vector used for cloning the reporter construct was obtained from Promega (pGL2-Basic, Promega Corp., Madison, WI) and was used as an empty vector control. A plasmid containing *Renilla* luciferase (pRL-CMV, Promega Corp., Madison, WI) was co-transfected as a control for transfection efficiency. R2FWT and R2FDD cells were plated in 35-mm tissue culture dishes and incubated in R2F medium overnight to reach 50–60% confluence the next day. Cells were then transfected using the Lipofectamine 2000 (Invitrogen) according to the manufacturer's protocol. Two μg of plasmid DNA were co-transfected with 0.15 μg of the *Renilla* luciferase plasmid in each dish. After 4–6 h of transfection, cells were supplemented either with R2F medium alone (diluent) or R2F medium with 40 μM p9-mer or 100 μM pTT. Cells were then incubated for 24 and 48 h at 37 °C in 5% $CO_2$ before harvesting for dual-luciferase assay. Promoter activity was then assayed using a dual-luciferase reporter assay system (Promega Corp., Madison, WI) according to the manufacturer's protocol. Firefly luciferase values were corrected for transfection efficiency according to *Renilla* luciferase values

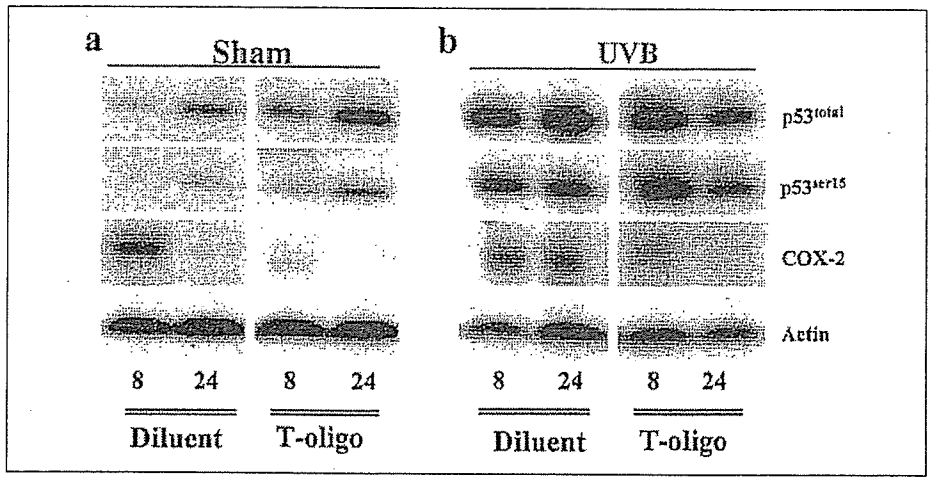


FIGURE 1. **T-oligo pretreatment up-regulates and activates p53 and down-regulates constitutive and UV light-induced COX-2 expression.** Human fibroblasts were pretreated once with diluent or T-oligo (p9-mer 40 μM; pTT data not shown) for 48 h. *a*, paired dishes were then sham-irradiated and harvested after 8 and 24 h and processed for Western blot analysis to evaluate the expression of COX-2, $p53^{total}$, $p53^{Ser15}$, and actin (loading control). Between 8 and 24 h, T-oligo pretreatment down-regulated constitutive COX-2 expression, which was inversely related to up-regulation of $p53^{total}$ and $p53^{Ser15}$ levels. These experiments were repeated three times with similar results. *b*, paired dishes were then UVB-irradiated with 15 mJ/cm², harvested, and then processed as for *a*. In diluent-treated UV light-irradiated samples, $p53^{total}$ and $p53^{Ser15}$ levels increased from 8 to 24 h, whereas in T-oligo-treated UV light-irradiated cells, $p53^{total}$ and $p53^{Ser15}$ expression was greater at 8 h. This earlier and higher up-regulation and activation of p53 in T-oligo-treated UV light-irradiated cells were accompanied by a striking decrease at 8 h and virtually complete inhibition of UV light-induced COX-2 expression in T-oligo-treated *versus* diluent-treated control cells. Similar results were obtained in three independent experiments with no difference between p9-mer and pTT results.

and revealed minimal differences in transfection efficiency among dishes. Luciferase activity was then expressed as percent of diluent value, setting diluent as 100%.

*Immunoprecipitation and Immunoblotting*—Cell lysates were precleaned with protein G-Sepharose beads for 2 h at 4 °C. Then 100 μg of total cell proteins were incubated with 2 μg of monoclonal p300 antibodies (GeneTex® Inc., San Antonio, TX), followed by the addition of protein G-Sepharose beads. The immunoprecipitated products were then subjected to SDS-PAGE and Western blot analysis as described (62). After transferring proteins to nitrocellulose membrane antibody reactions were performed with NFκB (p65) antibodies and p53 (DO-1) (both from Santa Cruz Biotechnology).

*Human Skin Explant Studies*—Human skin fragments from healthy donors (aged 56 ± 15 years, mean ± S.D.) were brought to the laboratory within 30 min after excision during plastic or facial reconstructive surgery. After removing subcutaneous fat and deep dermis, skin was cut into 5 × 5-mm squares and placed in 60-mm tissue culture dishes. Paired skin explants were then incubated in either medium alone or medium supplemented with 100 μM pTT or 40 μM p9-mer for 24 h. Medium consisted of Dulbecco's modified Eagle's medium with 10% calf serum plus KBM-2 with growth factors (50/50 v/v). The skin explants were then irradiated with a single dose of 30 mJ/cm² UVB. One set was sham-irradiated as a negative control. For each treatment, one explant was harvested immediately after UVB irradiation. The dishes were then re-fed with fresh medium lacking T-oligos, and explants were harvested at 6, 18, and 24 h after UVB irradiation. Harvested skin was snap-frozen at −80 °C in OCT medium for later processing.

*Immunohistochemistry and Immunofluorescence*—Snap-frozen human skin explants were processed for staining by cutting 4–6-μm sections and fixing them in acetone for 10 min at −20 °C. COX-2 staining was performed using the Ultravision Detection System (TQ-015-HA, Labvision Corp., Fremont, CA) according to manufacturer's protocol. Primary antibodies used included anti-COX-2 (Santa Cruz Biotechnology), human anti-p53 DO-7 (DakoCytomation, Carpinteria, CA), and anti-phospho-$p53^{Ser15}$ (Cell Signaling Technology, Beverly, MA). For the p53 DO-7 and $p53^{Ser15}$ stainings, sections were blocked in 10% goat normal serum in Tris-buffered saline for 15 min at room temperature and then incubated with primary antibody overnight at 4 °C. Sections were then washed in Tris-buffered saline three times for 5 min each before being incubated with the appropriate fluorescein isothiocyanate-labeled secondary antibody at 37 °C for 45 min. Finally, sections were washed as before and mounted with Vectashield mounting medium containing 4′,6-diamidino-2-phenylindole to visualize nuclei and were stored at −20 °C. We delineated ≈10-μm × 1-mm areas using computer-assisted image analysis and counted $p53^{total}$ and $p53^{Ser15}$ (+) nuclei in the epidermis. For each time point we analyzed an average of three randomly selected visual fields of $p53^{total}$ and $p53^{Ser15}$-stained epidermis from three to five donors per treatment condition. To avoid bias all counts were done by a single investigator for whom all samples were blinded by another investigator.

*Statistical Analysis*—Difference in protein expression, Cox-2 promoter activity, and $p53^{total}$ and $p53^{Ser15}$ (+) nuclei in T-oligo *versus* control-treated samples were analyzed by the analysis of variance post hoc analysis using the StatView statistical program (SAS Institute, Gary, NC). Groups were considered different when $p < 0.05$ (50).

## RESULTS

*T-oligo Pretreatment Down-regulates Base-line and UVB-induced COX-2 Protein Levels That Coincide with Up-regulation and Activation of p53 Levels*—The effect of T-oligo pretreatment on constitutive and UV light-induced levels of COX-2 and p53 was examined by Western blot analysis (Fig. 1), and results were confirmed by densitometric analysis of the blots (Fig. S1). In diluent-treated sham-irradiated cells, the constitutive $p53^{total}$ and $p53^{Ser15}$ levels were negligible at 8 h and moderately increased 24 h later (Fig. 1*a* and Fig. S1, *a* and *b*), consistent with approaching confluence of the cultures.[6] Reciprocally, COX-2 was constitutively expressed in diluent-treated sham-irradiated samples at 8 h and decreased by 24 h (Fig. 1*a* and Fig. S1*c*). In comparison, in T-oligo-treated sham-irradiated cells, COX-2 protein levels were strikingly lower at 8 h and virtually undetectable at 24 h, time points 56 and 72 h after T-oligo supplementation (Fig. 1*a* and Fig. S1*c*), suggesting that T-oligo treatment for 48 h down-regulates constitutive COX-2 levels in human fibroblasts. These decreases in COX-2 protein level were

[6] V. Marwaha, B. A. Gilchrest, and D. A. Goukassian, unpublished observations.

inversely related to the increases in both $p53^{total}$ and $p53^{Ser15}$ in T-oligo-treated sham-irradiated cells (Fig. 1*a* and Fig. S1, *a* and *b*).

UV irradiation up-regulated $p53^{total}$ and $p53^{Ser15}$ levels by 8 h and through 24 h and up-regulated COX-2 within 24 h, as reported previously (25, 50, 55), in diluent-treated cells (Fig. 1*b* and Fig. S1, *d–f*). T-oligo-treated cells also showed UV light-induced increases in $p53^{total}$ and $p53^{Ser15}$, with both sham- and UV light-induced levels markedly higher than in diluent-treated controls, as expected (55). As also expected if active p53 negatively regulates COX-2 levels, in T-oligo-treated cells COX-2 was virtually undetectable by 24 h after UVB (Fig. 1*b* and Fig. S1*f*), the time of maximal UV light-induced COX-2 protein expression reported by others (27, 63). After UV irradiation, maximal p53 induction and activation are reported to occur at ~2–24 h (depending on UV light dose) (64). Because T-oligo pretreatment appeared to accelerate the time of peak, UV light induction and activation of p53 as well as to increase the magnitude of p53 induction and activation (Fig. 1), we examined a more detailed time course, harvesting fibroblasts pretreated with T-oligo or diluent alone for 48 h immediately after UV irradiation and after 4, 6, 8, 16, and 24 h (Fig. S2). Consistent with our interpretation of the experiment shown in Fig. 1, diluent-pretreated cells showed peak phospho-$p53^{Ser15}$ induction at 6 – 8 h, with a return to base-line by 24 h, whereas T-oligo-pretreated cells had ~85% higher phospho-$p53^{Ser15}$ levels immediately post-irradiation and had tripled this induction within 4 h of an ~3-fold increase that gradually declined through 24 h (Fig. S2). Total p53, in contrast to activated p53, showed similar patterns in both T-oligo and diluent pretreated fibroblasts with substantial inductions by 4 h of post-UV light that declined only slightly by 24 h. However, in diluent-pretreated cells, $p53^{total}$ levels were far lower (~4-fold) of $p53^{total}$ levels in T-oligo-pretreated cells (Fig. S2). In combination, these data are consistent with a delayed direct effect of T-oligos on COX-2 expression, such as altered transcription rate subsequently reflected in protein levels. Alternatively or in addition, this may indicate involvement of an subsequent event downstream of p53 activation, such as p53-mediated inhibition of a known positive COX-2 transcriptional regulator, such as NFκB, NF-IL6, or AP1 (65–67).

*T-oligo Pretreatment Down-regulates COX-2 through p53-dependent Repression of COX-2 Promoter*—To evaluate further the involvement of p53 in T-oligo-induced down-regulation of COX-2 expression, we performed transient transfection studies using two isogenic fibroblast cell lines, one that expresses WT p53 (R2FWT) and one that is permanently transfected with dominant negative p53 (R2FDD) (52–54).

As shown by Western blot analysis and quantification by densitometry, R2FDD cells expressed higher constitutive levels of $p53^{total}$ and $p53^{Ser15}$ than R2FWT cells (~6- and or 40-fold, respectively), as expected (54), and showed virtually no T-oligo-induced up-regulation of either $p53^{total}$ or $p53^{Ser15}$ (Fig. 2*a* and Fig. S3a), whereas in R2FWT cells by 24 h T-oligo induced a more than 5-fold increase in $p53^{Ser15}$ and a 37% increase in $p53^{total}$ levels (Fig. 2*a* and Fig. S3*b*).

To verify that the p53 status of the cell lines had not changed over time in culture, we next evaluated T-oligo-induced p53 DNA binding activity. EMSA showed that in T-oligo-treated R2FDD cells, consensus sequence binding was minimal and did not increase over time, whereas in contrast binding in R2FWT cells was far higher as early as 8 h and was maximal by 24 h (Fig. 2*b*). These data confirm the reported p53 status in the R2FWT *versus* R2FDD cells.

The transcription factor NFκB is a known positive regulator of *COX-2* gene expression (68). Because recent reports indicate that activation of p53 by various stimuli inhibits NFκB activity (69, 70), we next evaluated NFκB DNA binding to its consensus sequence after T-oligo treatment. In both R2FWT and R2FDD cells that received T-oligos in fresh medium, NFκB binding decreased between 1.5 and 8 h and then increased again by 16 h (Fig. 2*c*), consistent with the known serum-mediated bi-phasic increase in NFκB activity (71–73). However, by 24 h, the time of maximal p53 activation in R2FWT cells (Fig. 2*b*), there was a marked decrease in NFκB binding activity compared with R2FDD cells (Fig. 2*c*), suggesting that p53 activation inhibited NFκB DNA binding activity after T-oligo treatment.

We then evaluated the effect of T-oligos on NFκB-driven transcription by transfecting R2FWT and R2FDD cells with an NFκB reporter plasmid. In cells expressing $p53^{WT}$, within 24 h T-oligo treatment decreased NFκB-driven transcription by ~35%, whereas in $p53^{DN}$ cells T-oligo treatment had no inhibitory effect on NFκB-driven transcription (Fig. 2*d*). We next transfected these cells with the COX-2 reporter plasmid. In R2FWT cells, treatment with T-oligos decreased COX-2 transcription by more than 50%, whereas in R2FDD cells T-oligo treatment had virtually no effect (Fig. 2*e*). In combination, these results demonstrate that functional p53 is required for T-oligo-induced repression of the COX-2 promoter and suggest that the effect may be mediated at least in part through NFκB.

To examine if T-oligo-induced p53-mediated repression of the COX-2 promoter depends on inhibition of NFκB transcriptional activity, we evaluated the effect of T-oligo treatment on NFκB-driven transcription by transfecting R2FWT and R2FDD cells with the COX-2 gene promoter with a site-specific mutation of the NFκB binding region (see diagram in Fig. S4*a*). In R2FWT cells transfected with WT COX-2 promoter, treatment with T-oligos decreased COX-2 transcription by more than 70%, whereas in R2FWT cells transfected with the mutated COX-2 promoter, T-oligo treatment had no inhibitory effect (Fig. S4*b*). In R2FDD cells, transfected with either WT or NFκB mutant COX-2 plasmid, T-oligo treatment had no effect (data not shown). These data demonstrate direct involvement of NFκB in T-oligo-induced p53-mediated repression of COX-2 promoter.

*T-oligo Pretreatment Down-regulates Base-line and UVB-induced COX-2 Protein Levels in Human Keratinocytes, Coinciding with Activation of p53, p53-dependent Inhibition of NFκB Activity, and NFκB-dependent Transactivation*—Because keratinocytes are a primary target for UVB damage and are the cells that give rise to UV light-induced actinic keratoses and SCC, we also examined the effect of T-oligos on primary human keratinocytes. Keratinocytes were pretreated with either T-oligos or diluent alone for 48 h and then sham or UV light-irradiated. Cells were then placed in medium without T-oligos and harvested for analysis of COX-2 protein levels and p53 DNA binding activity 8 and 24 h after irradiation. As shown by Western blot analysis (Fig. 3*a*) and quantified by densitometry (Fig. S5) in sham-irradiated keratinocytes, constitutive COX-2 expression was low at 8 and 24 h and similar in diluent-treated *versus* T-oligo-treated cells.

As reported previously (27, 74), UV irradiation markedly up-regulated COX-2 within 24 h in diluent-treated control cells (Fig. 3*b* and Fig. S5). However, as expected if T-oligos negatively regulate COX-2 in keratinocytes as well as in fibroblasts, COX-2 levels in T-oligo-treated keratinocytes were reduced by >50% at both 8 and 24 h (Fig. 3*b* and Fig. S5), the time of maximal UV light-induced COX-2 protein expression reported by others in this cell type (27, 74).

To substantiate further the involvement of p53 in T-oligo-induced down-regulation of COX-2 expression in human keratinocytes, we next evaluated T-oligo-mediated changes in p53 DNA binding activity using the protein from the same samples that was used to evaluate COX-2 protein levels in keratinocytes. At 8 and 24 h, EMSA showed minimal p53 DNA binding activity in T-oligo-treated or diluent-treated sham-irradiated cells, similar to the negative control (Fig. 3*c*, *lanes 7–10 versus 2*). As expected, UV irradiation increased p53 binding activity in dilu-

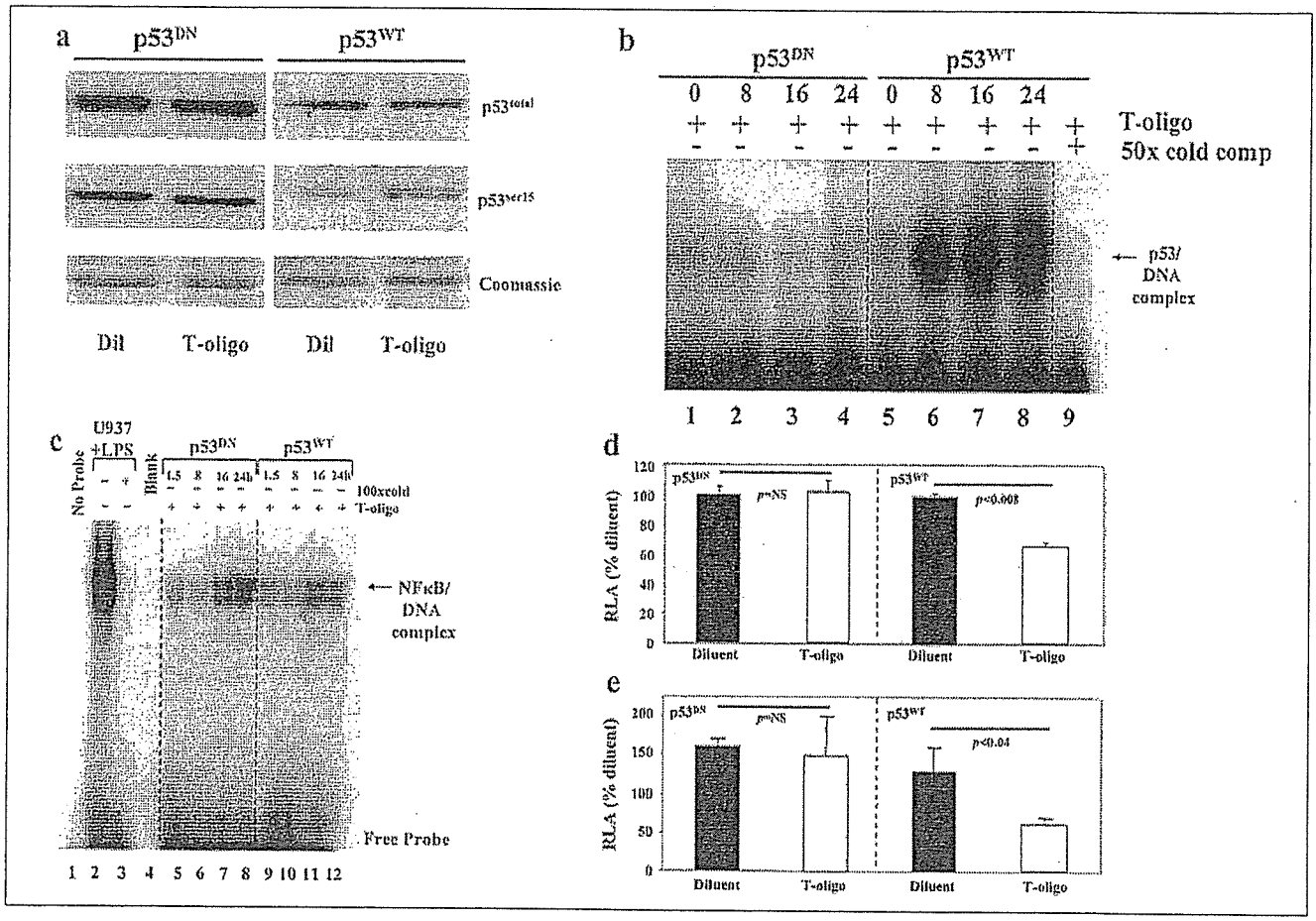


FIGURE 2. **T-oligo down-regulates COX-2 promoter activity through activation of p53.** R2FWT and R2FDD were additionally transiently transfected with a full-length COX-2 promoter-firefly luciferase reporter construct. *a*, cells treated once 48 h after transfection with either diluent or T-oligo (p9-mer 40 μM) and then processed for Western blot analysis after 24 h. In R2WT cells, T-oligo increased $p53^{Ser15}$ levels and minimally increased $p53^{total}$ levels compared with diluent treatment. However, in R2FDD cells, there was a high base-line expression of $p53^{total}$ and $p53^{Ser15}$ with no up-regulation by T-oligo. *b*, nuclear protein isolated from paired cultures 8, 16, and 24 h after addition of T-oligo (p9-mer 40 μM) shows substantial p53 DNA binding activity only in R2FWT cells. Specificity of binding is confirmed by the disappearance of the band in the control lane of R2FWT cell lysate treated with T-oligos for 24 h, reacted with a 50× excess of cold probe. *c*, nuclear protein isolated from paired cultures after T-oligo (p9-mer 40 μM) addition in fresh medium showed a bi-phasic pattern of NFκB DNA binding activity in R2FDD as well as R2FWT cells, but at 24 h, the time of increased p53 activity in R2FWT cells, NFκB binding activity was markedly decreased. Specificity of binding is confirmed by lack of a band in the *control lane 3* reacted with a 100× excess of cold probe compared with the strong positive band in *lane 2* containing a nuclear extract of lipopolysaccharide (*LPS*)-treated U937 cells. *d*, all cells were co-transfected with a *Renilla* luciferase reporter, to normalize for transfection efficiency of the NFκB reporter plasmid or the empty vector pGL2, a negative control. Transfectants were treated once with either diluent or T-oligo for 24 h before harvesting for the dual luciferase assay. A set of cells was transfected with the empty vector used to create the NFκB reporter construct. Results shown are the average of three separate experiments in duplicate for relative luciferase activity (*RLA*) for the firefly *versus Renilla* luciferase in the same dishes. In R2FWT cells, T-oligo treatment (p9-mer 40 μM) decreased NFκB-driven transcription by ~34% (100 ± 3 *versus* 66 ± 4, $p < 0.008$, diluent *versus* T-oligo), but in R2FDD cells, treatment with T-oligo had no effect (100 ± 11 *versus* 102 ± 16, $p = 0.8$, diluent *versus* T-oligo). *e*, all cells were processed as described in *d* but were transfected with a COX-2 promoter construct. Results shown are the average of three separate experiments in triplicate with firefly luciferase values normalized against *Renilla* luciferase values in the same dishes. In R2FWT cells, T-oligo treatment (p9-mer 40 μM) decreased COX-2 promoter activity by ~50% (125 ± 30 *versus* 58 ± 8, $p < 0.04$, diluent *versus* T-oligo), but in the R2FDD cells, T-oligo treatment had no effect (100 ± 6 *versus* 94 ± 30, $p$ = not significant (*NS*), diluent *versus* T-oligo).

ent-treated keratinocytes between 8 and 24 h (Fig. 3*c*, *lanes 3 versus 5*). However, in T-oligo-treated UV light-irradiated keratinocytes, p53 binding activity was increased 4-fold as early as 8 h after UVB compared with the levels in diluent-treated UV light-irradiated cells (Fig. 3*c*, *lanes 4 versus 3*), although by 24 h p53 DNA binding activity was less and was comparable in diluent- *versus* T-oligo-treated UV light-irradiated samples (Fig. 3*c*, *lanes 6 versus 5*). These data confirm an inverse relationship between p53 activity and COX-2 levels in human keratinocytes, as well as in fibroblasts.

Because NFκB is a known positive regulator of COX-2 transcription and we found that T-oligo treatment inhibits NFκB DNA binding activity in fibroblasts, experiments were performed to confirm this presumptive mechanism for indirect T-oligo-mediated p53-dependent inhibition of COX-2 transcription in keratinocytes. We reasoned that a possible limiting factor for the transcriptional activity of both p53 and NFκB may be the binding to the transcriptional co-activator protein p300 (70, 75). To address this possibility, we pretreated human keratinocytes with diluent or T-oligo for 24 h. Cells were then UV light-irradiated with 15 mJ/cm$^2$ followed by incubation in medium without T-oligos for 8 and 24 h and harvested for immunoprecipitation with anti-p300 antibodies followed by Western blot analysis for NFκB/p65 and p53 (Fig. 3*d*). In diluent-treated UV light-irradiated keratinocytes, NFκB/p65 binding to p300 increased markedly between 8 and 24 h after UV irradiation (Fig. 3*d*, *lanes 1 versus 3*). In contrast, in T-oligo-pretreated UV light-irradiated keratinocytes, NFκB binding to p300 was decreased relative to control as early as 8 h, and by 24 h NFκB binding to p300 was virtually undetectable (Fig. 3*d* *lanes 2 versus 4*). These data strongly suggest that T-oligo treatment decreases NFκB transcriptional activity via reduction of NFκB binding to its transcriptional co-activator p300 protein. Consistent with this interpretation, the amount of p53 binding to p300 was strikingly increased in T-oligo-treated *versus* control cells at both 8 and 24 h (Fig. 3*d*, *lanes 1* and *3 versus 2* and *4*, respectively). These data are consistent with an indirect mechanism of T-oligo-mediated p53-dependent inhibition of NFκB transcriptional

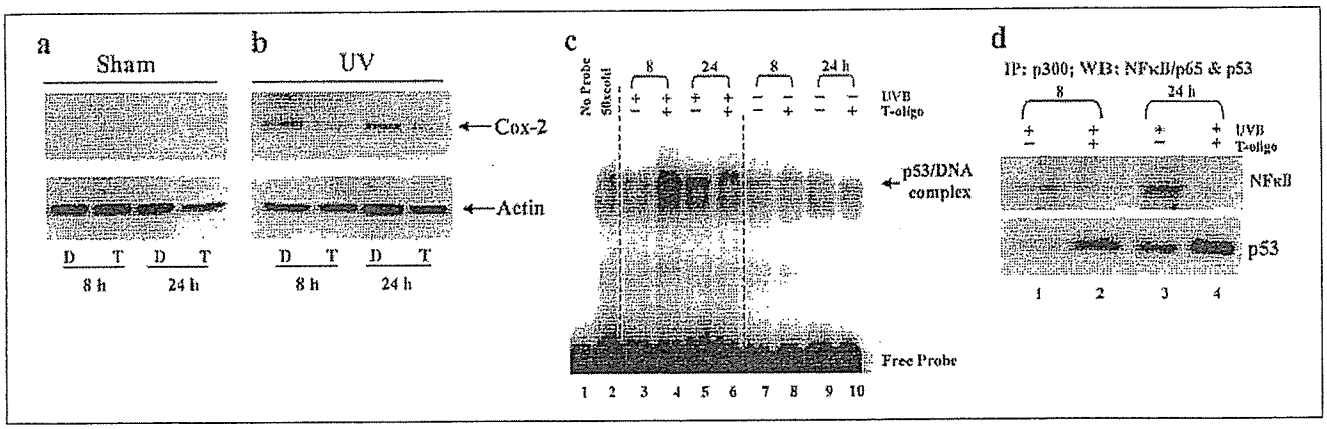


FIGURE 3. **T-oligo pretreatment activates p53 and down-regulates constitutive and UV light-induced COX-2 expression in keratinocytes.** Human newborn keratinocytes were treated as in Fig. 1. *a*, paired dishes were then sham-irradiated and harvested after 8 and 24 h for evaluation of COX-2 and actin (loading control) protein levels. These experiments were repeated two times with similar results. *b*, paired dishes were then UVB-irradiated with 15 mJ/cm$^2$, harvested, and processed as for *a*. At 8 h COX-2 expression was comparable in diluent-treated and T-oligo-treated samples. In UV light-irradiated control samples, COX-2 expression increased by 8 h with a further increase at 24 h, whereas in T-oligo-treated UV light-irradiated cells, COX-2 expression was significantly down-regulated throughout the 24 h. Similar results were obtained in three independent experiments. *c*, cells lysates from the same samples that were used to evaluate COX-2 protein levels in keratinocytes in *a* were used to evaluate T-oligo-mediated changes in p53 DNA binding activity in EMSA. Specificity of binding is confirmed by significant reduction of the band in the control lane using 50× excess of cold probe and protein lysate of keratinocytes treated with T-oligos for 8 h (*lane 2 versus lane 4*). *d*, cell lysates from the same samples that were used to evaluate COX-2 protein levels and p53 binding activity in keratinocytes in *b* and *c* (only T-oligo-treated UV light-irradiated) were used for immunoprecipitation (*IP*) with anti-p300 antibodies followed by Western blot analysis for NFκB/p65 and p53. T-oligo treatment decreased binding of NFκB to p300 by 8 h and was virtually undetectable by 24 h, whereas in T-oligo-treated UB-irradiated keratinocytes p53 binding to p300 was increased already by 8 h and was even greater by 24 h.

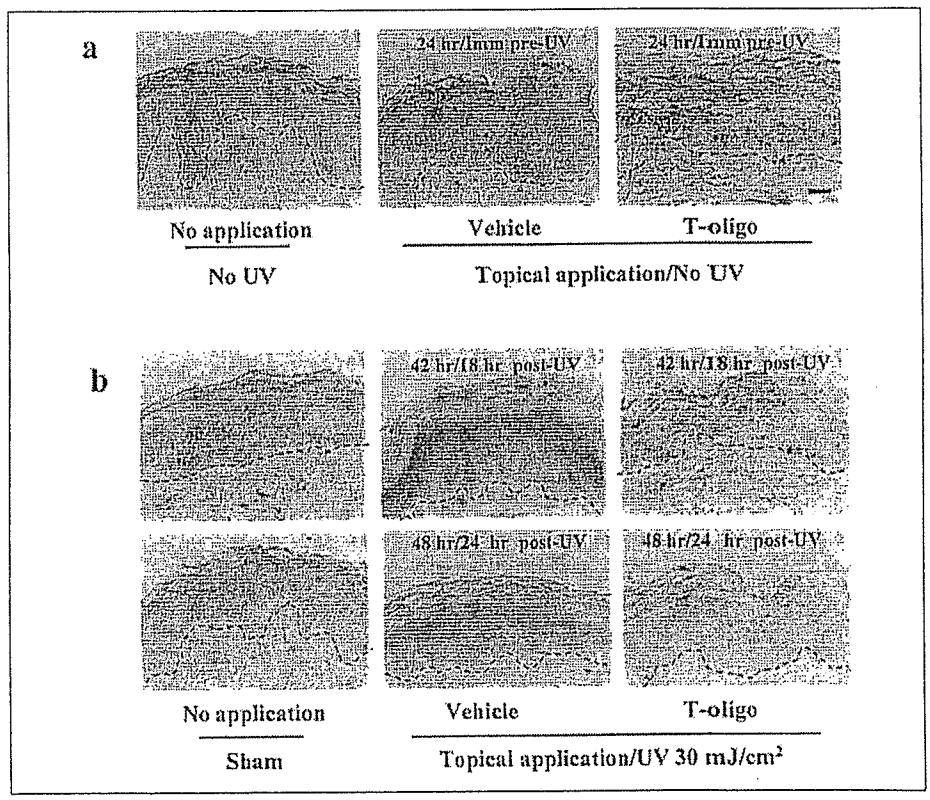


FIGURE 4. **T-oligo treatment decreases constitutive and UVB-induced COX-2 levels in human skin explants.** Human skin explants (10 per donor, 5 for each T-oligo) were prepared from otherwise discarded normal adult skin and treated immediately as described under "Experimental Procedures." Untreated nonirradiated skin showed constant low COX-2 expression over the 48-h experiment. *a*, in paired explants harvested after 24 h, T-oligos (pTT 100 μM; p9-mer data not shown) modestly decreased low base-line levels of COX-2 expression in the suprabasal epidermis. *b*, in paired explants harvested after T-oligo treatment and subsequent UVB irradiation, T-oligos strikingly decreased UVB-induced levels of COX-2 expression in the suprabasal epidermis as early as 18 h and continued through 24 h after irradiation. Specificity of COX-2 antibody staining was confirmed by staining sections of nontreated and diluent/T-oligo-treated and UVB-irradiated samples with mixed keratin human monoclonal mouse anti-human antibodies (DakoCytomation, Carpinteria, CA). No difference in epidermal staining pattern between nontreated and treated and then UV light-irradiated samples was detected, suggesting specificity of COX-2 antibody staining (Fig. S6, *a* and *b*). Dermal epidermal junction is indicated by the *dashed line*; ×200 magnification, all panels.

activity in which activated p53 successfully competes with NFκB for binding to their common co-activator, p300.

*T-oligo Pretreatment Down-regulates Both Base-line and UVB-induced COX-2 Expression in Human Explants*—The effect of T-oligos on COX-2 levels in human skin was studied using adult skin explants. Explants were treated as described under "Experimental Procedures" and then processed for immunostaining for COX-2, p53$^{total}$, and phospho-p53$^{Scr15}$ levels. COX-2 was constitutively expressed throughout the epidermis, particularly in the suprabasal layers, as reported previously (76). Pretreatment with T-oligos modestly down-regulated constitutive COX-2 levels (Fig. 4*a*) and strongly inhibited UV light-induced COX-2 levels (Fig. 4*b*). By 18 and 24 h after a single 30 mJ/cm$^2$ dose of UVB, there was a significant decrease in COX-2 immunostaining in T-oligo-treated skin treated once 42 or 48 h previously with T-oligo when compared with sham-irradiated untreated control skin. In contrast, in vehicle-treated skin there was a dramatic

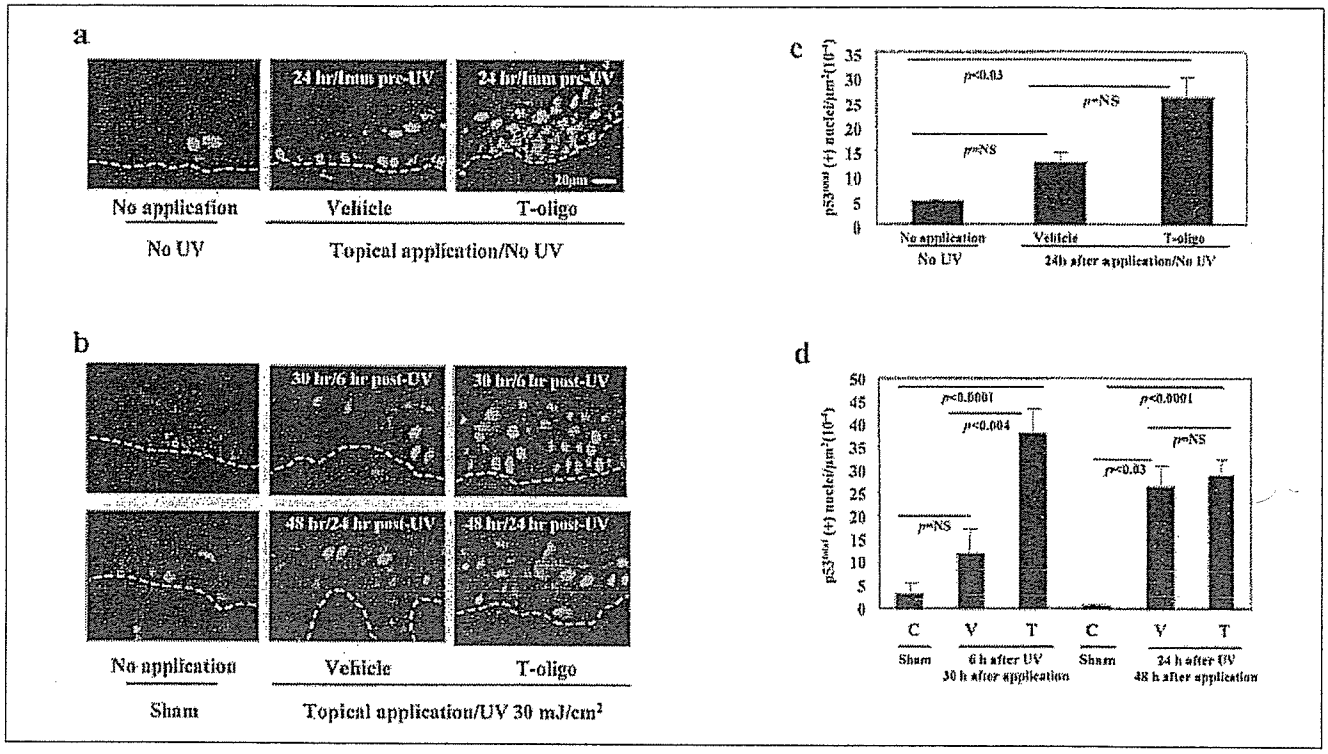


FIGURE 5. **T-oligo treatment increases constitutive and UVB-induced $p53^{total}$ levels in human skin.** Adjacent sections of the same explants shown in Fig. 4 were reacted with a fluorescently tagged antibody to total p53 and examined under a fluorescent microscope. There is no change in low p53 expression in untreated nonirradiated explants over the 48-h experiment. *a*, T-oligo (pTT 100 μM; p9-mer data not shown) increased constitutive levels of $p53^{total}$ expression, as shown by the number of positive (+) nuclei in the epidermis. *b*, T-oligo treatment increases UV light-induced $p53^{total}$ expression 6 h after UVB, but the number of (+) nuclei in T-oligo *versus* vehicle-treated explants is comparable after 24 h and far greater than in sham-irradiated control explants. *c* and *d*, quantitative analysis of $p53^{total}$ (+) nuclei as determined by blindly examining at least 3–5 fields (×200) and averaging. Values are expressed per $10^{-4}$ $\mu m^2$ of epidermal area and represent explants prepared from three donors. In addition, to confirm the validity of quantifying $p53^{total}$ (+) nuclei per $10^{-4}$ $\mu m^2$ of epidermal area, we also quantified $p53^{total}$ (+) nuclei per number of nuclei (4′,6-diamidino-2-phenylindole + cells). No difference in the relative expression of $p53^{total}$ (+) nuclei was found using either quantification method (Fig. S7, *a* and *b*). Note that after 24 h nonirradiated T-oligo-treated explants have p53 positivity comparable with that of UV light-irradiated explants. *C*, control; *V*, vehicle; *T*, T-oligo; *NS*, not significant. ×200 magnification in all panels.

increase in COX-2 immunostaining by 16 h that diminished slightly but persisted through 24 h (Fig. 4*b*).

*T-oligo-induced Inhibition of COX-2 Expression in Human Skin Is Associated with Up-regulation and Activation of p53 Protein*—To confirm our *in vitro* findings of an inverse relationship between T-oligo-induced decreases in constitutive and UV light-induced COX-2 levels and increases in p53 level and activity, adjacent sections of the same human tissue that were used for COX-2 immunostaining were processed for both $p53^{total}$ and $p53^{Ser15}$ immunofluorescent staining. In T-oligo-treated *versus* vehicle-treated skin after 24 h, there was a >100% increase in the number of constitutively $p53^{total}$ positive (+) nuclei (26 ± 4 *versus* 12 ± 2, $p < 0.09$) (Fig. 5, *a* and *c*). In UV light-irradiated samples by 6 h the numbers of $p53^{total}$ (+) nuclei in T-oligo-treated samples were increased more than 3-fold above vehicle controls (38 ± 5 *versus* 12 ± 6, $p < 0.004$), and more than 10-fold above sham-irradiated samples, whereas the modest and variable increase in UV light-irradiated control samples remained insignificant (Fig. 5, *b* and *d*). By 24 h, the numbers of $p53^{total}$ (+) nuclei were similar in T-oligo-*versus* diluent-treated UV light-irradiated skin samples (29 ± 4 *versus* 26 ± 5, $p = 0.6$) and more than 20-fold higher in both cases than in the sham-irradiated controls (Fig. 5, *b* and *d*).

T-oligo treatment minimally increased the number of nuclei with detectable constitutive $p53^{Ser15}$ levels (0.3 ± 0.2 *versus* 0.5 ± 0.2, vehicle *versus* T-oligo, $p = 0.09$) (Fig. 6, *a* and *c*). However, compared with vehicle-treated UV light-irradiated skin, there was a modest but statistically significant increase in the number of $p53^{Ser15}$ (+) nuclei in T-oligo-treated UV light-irradiated skin samples at 6 and 24 h (6 h, 10.3 ± 0.8 *versus* 14 ± 0.6, $p < 0.001$; and 24 h, 8.5 ± 0.9 *versus* 13 ± 0.6, vehicle *versus* T-oligo, $p < 0.001$) as well as striking and highly significant increases above sham-irradiated untreated samples in both cases (Fig. 5, *b* and *d*). Taken together with the data of COX-2 immunostaining (Fig. 4*b*), these results establish an *in vivo* relevance of the cause-and-effect inverse relationship between increased p53 levels and activity and decreased COX-2 levels in T-oligo-treated human fibroblasts and keratinocytes (Fig. 1, *a* and *b*, and Fig. 3, *a–c*).

## DISCUSSION

UV irradiation is the major environmental carcinogen for human skin (77, 78), initiating and promoting development of both melanoma and nonmelanoma skin cancers (79–81). Mechanisms that contribute to UV light-induced mutagenesis and carcinogenesis include inactivation of tumor suppressor genes and/or activation of oncogenes (82–84), events that may also lead to clonal expansion of affected cells (85–89). However, in recent years a great deal of evidence has emerged suggesting that UV light-induced inflammation also plays an important role in tumor promotion and progression (26, 90–93). In murine models of skin carcinogenesis, it has been shown that administration of nonsteroidal anti-inflammatory drugs, especially selective COX-2 inhibitors, reduces the prevalence and multiplicity of UV light-induced neoplasms (74, 92–95), strongly implying direct involvement of COX-2 in cutaneous carcinogenesis.

The present study demonstrates that topical application of telomere 3′-overhang homolog DNA oligonucleotides, collectively termed T-oligos, inhibits UV light-induced up-regulation of COX-2 *in vitro* and *ex*

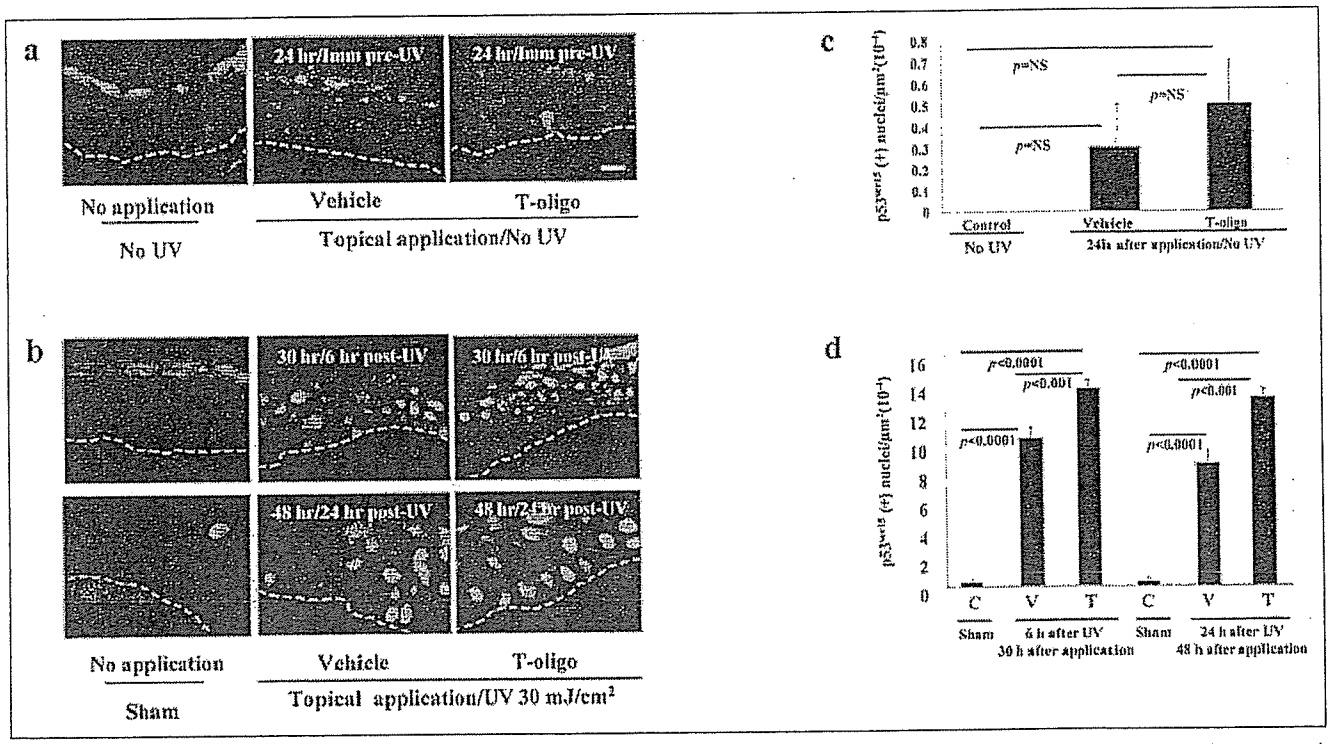


FIGURE 6. **T-oligos treatment increases constitutive and UVB-induced p53$^{Ser15}$ levels in human skin.** Adjacent sections of the same explants shown in Figs. 4 and 5 were reacted with a fluorescently tagged antibody to phospho-p53$^{Ser15}$ and then analyzed as described for Fig. 5. T-oligo (pTT 100 $\mu$M; p9-mer data not shown) treatment variably and minimally increased constitutive levels of p53$^{Ser15}$ expression (*a*) with the number of p53$^{Ser15}$ (+) nuclei in the epidermis consistently below 0.7 per $\mu m^2 \times 10^{-4}$ in all groups ($p$ = not significant (*NS*)). *c*, nonspecific retention of label in the stratum corneum was also observed in most specimens. After UV irradiation, the number of p53$^{Ser15}$ (+) nuclei increased dramatically compared with sham-irradiated controls within 6 h and through 24 h for both T-oligo- and vehicle-treated explants. *b*, quantitative analysis of p53$^{Ser15}$ (+) nuclei performed as for Fig. 5 revealed a roughly 20–30-fold increase in p53$^{Ser15}$ above preirradiation levels for both vehicle-treated and T-oligo-treated explants, with T-oligo-treated explants showing ~40 and 53% higher numbers of (+) nuclei at 6 and 24 h, respectively, a significant difference ($p < 0.001$) at both times (*d*). ×200 magnification, *a* and *b*, *upper panel*; ×400 magnification, *b*, *lower panel*.

*vivo* in human skin. These data expand our earlier reports that T-oligos elicit UV light-protective and cancer-preventative responses in skin cells (40, 45, 46, 50, 51). Most if not all of these responses are mediated at least in part through up-regulation and activation of p53, with subsequent effects on p53-regulated downstream target genes (49–51, 55, 56). Our current data show that T-oligo-dependent UV light-protective responses can be mediated specifically by transcriptional repression of gene products such as the inducible isoform of cyclooxygenase, COX-2 (17), that catalyzes the rate-limiting step of prostaglandin and thromboxane production (18–20). Western blot analysis of normal human fibroblasts and keratinocytes showed an inverse relationship between p53 up-regulation and activation and down-regulation of constitutive and UV light-induced COX-2 levels in both cell types. Studies in paired isogenic fibroblast lines with wild type *versus* dominant negative p53 confirmed that p53 transcriptional activity is required for this effect on COX-2. In addition, the present study also demonstrates that T-oligo addition to human skin explants up-regulates and activates constitutive p53 and, after subsequent UV light exposure, blocks COX-2 overexpression.

We demonstrate that T-oligos decrease COX-2 levels at least in part by decreasing COX-2 transcription, an effect that is dependent on p53 activity, not on total p53 levels. It is known that p53 suppresses a variety of promoters that contain one or more TATA boxes (96, 97). It was suggested that p53 suppresses gene expression by interfering with formation of the transcription preinitiation complex with TATA-binding proteins (TBPs) by preventing binding of TBPs to the TATA motif (98). Many genes are reported to be negatively regulated by p53. These include c-*Fos*, c-*Jun*, c-*Myc*, *IL-6*, heat shock protein 70 gene (*HSP70*), multidrug resistance gene (*MDR1*), and B-cell lymphoma gene-2 (*Bcl2*) (98–103).

Relevant to p53-dependent regulation of COX-2, it was shown that p53 inhibits the formation of complexes between TBPs and the murine and human COX-2 promoters in a cell-free system (33). The same authors also reported that wild type but not temperature-sensitive mutant p53 competed with TATA-binding proteins for binding to the mouse and human COX-2 promoters over a 100-bp segment surrounding the transcription initiation start on COX-2 promoter (33). Accordingly, to test the hypothesis that T-oligo-mediated p53-dependent suppression of COX-2 depends on repression of COX-2 promoter activity by activated p53, we tested T-oligo effect in p53$^{WT}$ *versus* p53$^{DN}$ cells. In cells expressing p53$^{WT}$, treatment with T-oligos decreased constitutive COX-2 promoter-driven transcription of a reporter plasmid by 54%, whereas in p53$^{DN}$ cells T-oligo treatment had virtually no effect on COX-2 promoter activity, demonstrating that functional p53 is required for T-oligo-induced repression of the COX-2 promoter. Our findings may also resolve apparently conflicting data in the literature concerning regulation of *COX-2* gene expression by p53, as investigators reporting positive p53 regulation of COX-2 in various mutant and tumor-derived cell lines correlated only the level of expression of the two proteins and did not assess p53 activity (104).

Cellular responses to DNA-damaging stimuli, including UV irradiation, are usually complex and often regulated by more than one transcription factor, for example by both p53 and NFκB (105). Furthermore, several studies have established a reciprocal inhibitory regulation of the transcription factors NFκB and p53 in various cell lines treated with DNA-damaging agents, mediated through competitive binding of p53 and NFκB to the transcriptional co-activator p300 protein (69, 70, 106). We found that in human fibroblasts and keratinocytes, T-oligo treat-

ment up-regulates and activates p53, coinciding with decreased NFκB DNA binding activity and inhibition of transcription from NFκB-driven promoter constructs. Moreover, in human keratinocytes we also showed that treatment with T-oligo prior to UV irradiation inhibited p300 binding to NFκB and increased p300 binding to p53, as shown by immunoprecipitation of p300, followed by Western blot for NFκB/p65 and p53 proteins, coinciding with p53 activation and decreased COX-2 expression. This second and indirect mechanism of inhibition of COX-2 expression may explain the somewhat delayed T-oligo-mediated inhibition of COX-2 expression observed in our studies. Alternatively or in addition, the detailed regulation of COX-2 may also depend on the stimulus, cell type, and tissue environment, leading to predominant/selective regulation of the COX-2 promoter at different times by such known positive transcription factors as AP1, NF-IL6, NFκB, NFAT, and PEA3 (19). In fact, in our previous publications we have shown that T-oligos appear to exert their protective effects by activating ATM kinase (38) and its downstream effectors, including p53 and p95/Nbs1 (38, 40, 49), as well as by up-regulating a variety of other genes including *E2F1*, $p16^{INK4a}$, and the *p53* homologue *p73* not known to be regulated by ATM (38–40, 49, 55).

E2F1 may be of particular relevance to our findings, as there is evidence suggesting E2F1 mediated inhibition of NFκB in various cell types (107, 108). Indeed, Tanaka *et al.* (107) showed that endogenous E2F1 competes with NFκB/p50 for binding to the p65 subunit of NFκB and that this physical interaction of E2F1/p65 inhibits NFκB transcriptional activities. Additionally, Phillips *et al.* (109) have shown in Saos2 cells lacking p53 that E2F1-induced inhibition of NFκB nuclear translocation and activity is mediated by the abrogation of TRAF-2 protein and inhibition of IκB kinase phosphorylation. It will be of interest to further investigate, specifically in cells with nonfunctional p53, such as the majority of UV light-induced skin neoplasms, whether T-oligo-mediated E2F1-dependent inhibition of NFκB in the absence of functional p53 may also inhibit COX-2 expression.

To date, attention has been directed toward inhibition of COX-2 enzyme activity, and much less attention has been given to modulation of COX-2 protein levels that are constitutively increased in many tumor cells (110). However, compared with young skin, there is an age-associated increase in constitutive and UV light-induced prostaglandin $E_2$ production and COX-2 expression in human skin (26). The resulting chronic low grade inflammation may have crucial pathophysiologic implications for many aging processes, such as loss of collagen, and may contribute to the development and progression of age-associated diseases, including malignancies. Indeed, experimental COX-2 overexpression has been also reported to increase tumorigenesis in a variety of organ systems, including colon, lung, prostate, breast cancer, urinary bladder, pancreas, and liver (76, 111–115), in addition to skin (26–29). COX-2 overexpression is also increasingly implicated in the process of tumor angiogenesis (neovascularization) through increasing vascular endothelial growth factor levels as well as producing prostaglandins and thromboxanes that promote endothelial cell migration (18).

We conclude that T-oligo treatment beneficially affects multiple contributors to carcinogenesis; T-oligos transiently inhibit cell proliferation (38–41, 44–51, 55, 56), enhance DNA repair capacity (49–51), and decrease mutagenesis and photocarcinogenesis (51), as well as induce apoptosis and senescence of malignant cells (38, 40, 42, 43). In the present report we demonstrate that T-oligos also decrease constitutive and UV light-induced levels of COX-2, an inflammatory mediator strongly implicated in the processes of photocarcinogenesis, chemical and spontaneous carcinogenesis, and tumor angiogenesis (116–118). Furthermore, we suggest that T-oligos may also combat the tendency for chronic low grade inflammation that accompanies aging (26).

*Acknowledgments—We are grateful to Dr. Christina Wu and Cynthia Curry for their valuable assistance in promoter regulation studies and to Kathleen Huard and Daniella Adrien for assistance in preparation of the manuscript.*

REFERENCES


1. Jemal, A., Murray, T., Ward, E., Samuels, A., Tiwari, R. C., Ghafoor, A., Feuer, E. J., and Thun, M. J. (2005) *CA–Cancer J. Clin.* 55, 10–30
2. Albert, M. R., and Weinstock, M. A. (2003) *CA–Cancer J. Clin.* 53, 292–302
3. Geller, A. C., Zhang, Z., Sober, A. J., Halpern, A. C., Weinstock, M. A., Daniels, S., Miller, D. R., Demierre, M. F., Brooks, D. R., and Gilchrest, B. A. (2003) *J. Am. Acad. Dermatol.* 48, 34–41
4. Brash, D. E., and Ponten, J. (1998) *Cancer Surv.* 32, 69–113
5. Zoumpourlis, V., Solakidi, S., Papathoma, A., and Papaevangeliou, D. (2003) *Carcinogenesis* 24, 1159–1165
6. Patrick, M. H. (1977) *Photochem. Photobiol.* 25, 357–372
7. Wood, R. D. (1996) *Annu. Rev. Biochem.* 65, 135–167
8. de Gruijl, F. R., van Kranen, H. J., and Mullenders, L. H. (2001) *J. Photochem. Photobiol. B Biol.* 63, 19–27
9. Sterenborg, H. J., de Gruijl, F. R., and van der Leun, J. C. (1986) *Photodermatol.* 3, 206–214
10. Lavker, R. M., Gerberick, G. F., Veres, D., Irwin, C. J., and Kaidbey, K. H. (1995) *J. Am. Acad. Dermatol.* 32, 53–62
11. Remenyik, E., Wikonkal, N. M., Zhang, W., Paliwal, V., and Brash, D. E. (2003) *Oncogene* 22, 6369–6376
12. Aubin, F. (2003) *Eur. J. Dermatol.* 13, 515–523
13. Schwarz, T. (2002) *Photodermatol. Photoimmunol. Photomed.* 18, 141–145
14. Bielenberg, D. R., Bucana, C. D., Sanchez, R., Donawho, C. K., Kripke, M. L., and Fidler, I. J. (1998) *J. Invest. Dermatol.* 111, 864–872
15. Hruza, L. L., and Pentland, A. P. (1993) *J. Invest. Dermatol.* 100, 35S–41S
16. Furstenberger, G., Gross, M., and Marks, F. (1989) *Carcinogenesis* 10, 91–96
17. Brecher, A. R. (2002) *J. Drugs Dermatol.* 1, 44–47
18. Turini, M. E., and DuBois, R. N. (2002) *Annu. Rev. Med.* 53, 35–57
19. Dannenberg, A. J., and Subbaramaiah, K. (2003) *Cancer Cell* 4, 431–436
20. Parente, L., and Perretti, M. (2003) *Biochem. Pharmacol.* 65, 153–159
21. Howe, L. R., Subbaramaiah, K., Brown, A. M., and Dannenberg, A. J. (2001) *Endocr. Relat. Cancer* 8, 97–114
22. Castelao, J. E., Bart, R. D., 3rd, DiPerna, C. A., Sievers, E. M., and Bremner, R. M. (2003) *Ann. Thorac. Surg.* 76, 1327–1335
23. Marnett, L. J., and DuBois, R. N. (2002) *Annu. Rev. Pharmacol. Toxicol.* 42, 55–80
24. Ferrandez, A., Prescott, S., and Burt, R. W. (2003) *Curr. Pharm. Des.* 9, 2229–2251
25. Chen, W., Tang, Q., Gonzales, M. S., and Bowden, G. T. (2001) *Oncogene* 20, 3921–3926
26. Seo, J. Y., Kim, E. K., Lee, S. H., Park, K. C., Kim, K. H., Eun, H. C., and Chung, J. H. (2003) *Mech. Ageing Dev.* 124, 903–910
27. An, K. P., Athar, M., Tang, X., Katiyar, S. K., Russo, J., Beech, J., Aszterbaum, M., Kopelovich, L., Epstein, E. H., Jr., Mukhtar, H., and Bickers, D. R. (2002) *J. Photochem. Photobiol. B Biol.* 76, 73–80
28. Orengo, I. F., Gerguis, J., Phillips, R., Guevara, A., Lewis, A. T., and Black, H. S. (2002) *Arch. Dermatol.* 138, 751–755
29. Fischer, S. M., Conti, C. J., Viner, J., Aldaz, C. M., and Lubet, R. A. (2003) *Carcinogenesis* 24, 945–952
30. Muller-Decker, K., Neufang, G., Berger, I., Neumann, M., Marks, F., and Furstenberger, G. (2002) *Proc. Natl. Acad. Sci. U. S. A.* 99, 12483–12488
31. Ahmed, S., Rahman, A., Hasnain, A., Lalonde, M., Goldberg, V. M., and Haqqi, T. M. (2002) *Free Radic. Biol. Med.* 33, 1097–1105
32. Ospina, J. A., Brevig, H. N., Krause, D. N., and Duckles, S. P. (2004) *Am. J. Physiol.* 286, H2010–H2019
33. Subbaramaiah, K., Altorki, N., Chung, W. J., Mestre, J. R., Sampat, A., and Dannenberg, A. J. (1999) *J. Biol. Chem.* 274, 10911–10915
34. Gallo, O., Schiavone, N., Papucci, L., Sardi, I., Magnelli, L., Franchi, A., Masini, E., and Capaccioli, S. (2003) *Am. J. Pathol.* 163, 723–732
35. Griffith, J. D., Comeau, L., Rosenfield, S., Stansel, R. M., Bianchi, A., Moss, H., and de Lange, T. (1999) *Cell* 97, 503–514
36. Stansel, R. M., de Lange, T., and Griffith, J. D. (2001) *EMBO J.* 20, 5532–5540
37. Karlseder, J., Broccoli, D., Dai, Y., Hardy, S., and de Lange, T. (1999) *Science* 283, 1321–1325
38. Eller, M. S., Li, G. Z., Firoozabadi, R., Puri, N., and Gilchrest, B. A. (2003) *FASEB J.* 17, 152–162
39. Li, G. Z., Eller, M. S., Firoozabadi, R., and Gilchrest, B. A. (2003) *Proc. Natl. Acad. Sci. U. S. A.* 100, 527–531
40. Eller, M. S., Puri, N., Hadshiew, I. M., Venna, S. S., and Gilchrest, B. A. (2002) *Exp.*

*Cell Res.* 276, 185–193
41. Hadshiew, I. M., Eller, M. S., Gasparro, F. P., and Gilchrest, B. A. (2001) *J. Dermatol. Sci.* 25, 127–138
42. Puri, N., Eller, M. S., Byers, H. R., Dykstra, S., Kubera, J., and Gilchrest, B. A. (2004) *FASEB J.* 18, 1373–1381
43. Li, G. Z., Eller, M. S., Hanna, K., and Gilchrest, B. A. (2004) *Exp. Cell Res.* 301, 189–200
44. Pedeux, R., Al-Irani, N., Marteau, C., Pellicier, F., Branche, R., Ozturk, M., Ranchi, J., and Dore, J. F. (1998) *J. Invest. Dermatol.* 111, 472–477
45. Eller, M. S., Yaar, M., and Gilchrest, B. A. (1994) *Nature* 372, 413–414
46. Eller, M. S., Ostrom, K., and Gilchrest, B. A. (1996) *Proc. Natl. Acad. Sci. U. S. A.* 93, 1087–1092
47. Curiel-Lewandrowski, C., Venna, S. S., Eller, M. S., Cruikshank, W., Dougherty, I., Cruz, P. D., and Gilchrest, B. A. (2003) *Exp. Dermatol.* 12, 145–152
48. Cruz, P. D., Jr., Leverkus, M., Dougherty, I., Gleason, M. J., Eller, M., Yaar, M., and Gilchrest, B. A. (2000) *J. Invest. Dermatol.* 114, 253–258
49. Eller, M. S., Maeda, T., Magnoni, C., Atwal, D., and Gilchrest, B. A. (1997) *Proc. Natl. Acad. Sci. U. S. A.* 94, 12627–12632
50. Goukassian, D. A., Bagheri, S., el-Keeb, L., Eller, M. S., and Gilchrest, B. A. (2002) *FASEB J.* 16, 754–756
51. Goukassian, D. A., Helms, E., van Steeg, H., van Oostrom, C., Bhawan, J., and Gilchrest, B. A. (2004) *Proc. Natl. Acad. Sci. U. S. A.* 101, 3933–3938
52. Tubo, R. A., and Rheinwald, J. G. (1987) *Oncogene Res.* 1, 407–421
53. Shaulian, E., Zauberman, A., Ginsberg, D., and Oren, M. (1992) *Mol. Cell. Biol.* 12, 5581–5592
54. Rheinwald, J. G., Hahn, W. C., Ramsey, M. R., Wu, J. Y., Guo, Z., Tsao, H., De Luca, M., Catricala, C., and O'Toole, K. M. (2002) *Mol. Cell. Biol.* 22, 5157–5172
55. Goukassian, D. A., Eller, M. S., Yaar, M., and Gilchrest, B. A. (1999) *J. Invest. Dermatol.* 112, 25–31
56. Maeda, T., Eller, M. S., Hedayati, M., Grossman, L., and Gilchrest, B. A. (1999) *Mutat. Res.* 433, 137–145
57. Gilchrest, B. A., Zhai, S., Eller, M. S., Yarosh, D. B., and Yaar, M. (1993) *J. Invest. Dermatol.* 101, 666–672
58. Werninghaus, K., Handjani, R. M., and Gilchrest, B. A. (1991) *Photodermatol. Photomed.* 8, 236–242
59. Kishore, R., Spyridopoulos, I., Luedemann, C., and Losordo, D. W. (2002) *Circ. Res.* 91, 307–314
60. Inoue, H., Yokoyama, C., Hara, S., Tone, Y., and Tanabe, T. (1995) *J. Biol. Chem.* 270, 24965–24971
61. Inoue, H., Taba, Y., Miwa, Y., Yokota, C., Miyagi, M., and Sasaguri, T. (2002) *Arterioscler. Thromb. Vasc. Biol.* 22, 1415–1420
62. Kishore, R., Luedemann, C., Bord, E., Goukassian, D., and Losordo, D. W. (2003) *Circ. Res.* 93, 932–940
63. Athar, M., An, K. P., Morel, K. D., Kim, A. L., Aszterbaum, M., Longley, J., Epstein, E. H., Jr., and Bickers, D. R. (2001) *Biochem. Biophys. Res. Commun.* 280, 1042–1047
64. Hall, P. A., McKee, P. H., Menage, H. D., Dover, R., and Lane, D. P. (1993) *Oncogene* 8, 203–207
65. Ramsay, R. G., Ciznadija, D., Vanevski, M., and Mantamadiotis, T. (2003) *Int. J. Immunopathol. Pharmacol.* 16, 59–67
66. Perfettini, J. L., Roumier, T., Castedo, M., Larochette, N., Boya, P., Raynal, B., Lazar, V., Ciccosanti, F., Nardacci, R., Penninger, J., Piacentini, M., and Kroemer, G. (2004) *J. Exp. Med.* 199, 629–640
67. Margulies, L., and Sehgal, P. B. (1993) *J. Biol. Chem.* 268, 15096–15100
68. Hung, J. H., Su, I. J., Lei, H. Y., Wang, H. C., Lin, W. C., Chang, W. T., Huang, W., Chang, W. C., Chang, Y. S., Chen, C. C., and Lai, M. D. (2004) *J. Biol. Chem.* 279, 46384–46392
69. Webster, G. A., and Perkins, N. D. (1999) *Mol. Cell. Biol.* 19, 3485–3495
70. Culmsee, C., Siewe, J., Junker, V., Retiounskaia, M., Schwarz, S., Camandola, S., El-Metainy, S., Behnke, H., Mattson, M. P., and Krieglstein, J. (2003) *J. Neurosci.* 23, 8586–8595
71. Rodel, F., Hantschel, M., Hildebrandt, G., Schultze-Mosgau, S., Rodel, C., Herrmann, M., Sauer, R., and Voll, R. E. (2004) *Int. J. Radiat. Biol.* 80, 115–123
72. Han, S. J., Ko, H. M., Choi, J. H., Seo, K. H., Lee, H. S., Choi, E. K., Choi, I. W., Lee, H. K., and Im, S. Y. (2002) *J. Biol. Chem.* 277, 44715–44721
73. Caba, E., and Bahr, B. A. (2004) *Acta Neuropathol.* 108, 173–182
74. Pentland, A. P., Scott, G., VanBuskirk, J., Tanck, C., LaRossa, G., and Brouxhon, S. (2004) *Cancer Res.* 64, 5587–5591
75. Ikeda, A., Sun, X., Li, Y., Zhang, Y., Eckner, R., Doi, T. S., Takahashi, T., Obata, Y., Yoshioka, K., and Yamamoto, K. (2000) *Biochem. Biophys. Res. Commun.* 272, 375–379
76. Buckman, S. Y., Gresham, A., Hale, P., Hruza, G., Anast, J., Masferrer, J., and Pentland, A. P. (1998) *Carcinogenesis* 19, 723–729
77. Miller, D. L., and Weinstock, M. A. (1994) *J. Am. Acad. Dermatol.* 30, 774–778
78. Scotto, J., and Fears, T. R. (1987) *Cancer Investig.* 5, 275–283
79. Giles, G. G., and Thursfield, V. J. (1996) *Cancer Forum* 20, 188–191
80. Gilchrest, B. A., Eller, M. S., Geller, A. C., and Yaar, M. (1999) *N. Engl. J. Med.* 340, 1341–1348
81. Sachs, D. L., Marghoob, A. A., and Halpern, A. (2001) in *Clinics in Geriatric Medicine* (Gilchrest, B. A., ed) Vol. 17, pp. 715–738, W. B. Saunders Co., Philadelphia
82. Osada, H., and Takahashi, T. (2002) *Oncogene* 21, 7421–7434
83. Kuper, H., Adami, H. O., and Trichopoulos, D. (2000) *J. Intern. Med.* 248, 171–183
84. Kopnin, B. P. (2000) *Biochemistry (Moscow)* 65, 2–27
85. Zhang, W., Remenyik, E., Zelterman, D., Brash, D. E., and Wikonkal, N. M. (2001) *Proc. Natl. Acad. Sci. U. S. A.* 98, 13948–13953
86. Brash, D. E., Ziegler, A., Jonason, A. S., Simon, J. A., Kunala, S., and Leffell, D. J. (1996) *J. Investig. Dermatol. Symp. Proc.* 1, 136–142
87. Aszterbaum, M., Epstein, J., Oro, A., Douglas, V., LeBoit, P. E., Scott, M. P., and Epstein, E. H., Jr. (1999) *Nat. Med.* 5, 1285–1291
88. Oro, A. E., Higgins, K. M., Hu, Z., Bonifas, J. M., Epstein, E. H., Jr., and Scott, M. P. (1997) *Science* 276, 817–821
89. McCormick, F. (1999) *Trends Cell Biol.* 9, 53–56
90. Vanderveen, E. E., Grekin, R. C., Swanson, N. A., and Kragballe, K. (1986) *Arch. Dermatol.* 122, 407–412
91. Cerutti, P. A., and Trump, B. F. (1991) *Cancer Cells* 3, 1–7
92. Fischer, S. M. (2002) *J. Environ. Pathol. Toxicol. Oncol.* 21, 183–191
93. Fischer, S. M., Lo, H. H., Gordon, G. B., Seibert, K., Kelloff, G., Lubet, R. A., and Conti, C. J. (1999) *Mol. Carcinog.* 25, 231–240
94. Pentland, A. P., Schoggins, J. W., Scott, G. A., Khan, K. N., and Han, R. (1999) *Carcinogenesis* 20, 1939–1944
95. Pentland, A. P. (2002) *Arch. Dermatol.* 138, 823–824
96. Mack, D. H., Vartikar, J., Pipas, J. M., and Laimins, L. A. (1993) *Nature* 363, 281–283
97. Ginsberg, D., Mechta, F., Yaniv, M., and Oren, M. (1991) *Proc. Natl. Acad. Sci. U. S. A.* 88, 9979–9983
98. Ragimov, N., Krauskopf, A., Navot, N., Rotter, V., Oren, M., and Aloni, Y. (1993) *Oncogene* 8, 1183–1193
99. Santhanam, U., Ray, A., and Sehgal, P. B. (1991) *Proc. Natl. Acad. Sci. U. S. A.* 88, 7605–7609
100. Wang, Q., and Beck, W. T. (1998) *Cancer Res.* 58, 5762–5769
101. Agoff, S. N., Hou, J., Linzer, D. I., and Wu, B. (1993) *Science* 259, 84–87
102. Miyashita, T., Harigai, M., Hanada, M., and Reed, J. C. (1994) *Cancer Res.* 54, 3131–3135
103. Kley, N., Chung, R. Y., Fay, S., Loeffler, J. P., and Seizinger, B. R. (1992) *Nucleic Acids Res.* 20, 4083–4087
104. Han, J. A., Kim, J. I., Ongusaha, P. P., Hwang, D. H., Ballou, L. R., Mahale, A., Aaronson, S. A., and Lee, S. W. (2002) *EMBO J.* 21, 5635–5644
105. Campbell, K. J., Chapman, N. R., and Perkins, N. D. (2001) *Biochem. Soc. Trans.* 29, 688–691
106. Ravi, R., Mookerjee, B., van Hensbergen, Y., Bedi, G. C., Giordano, A., El-Deiry, W. S., Fuchs, E. J., and Bedi, A. (1998) *Cancer Res.* 58, 4531–4536
107. Tanaka, H., Matsumura, I., Ezoe, S., Satoh, Y., Sakamaki, T., Albanese, C., Machii, T., Pestell, R. G., and Kanakura, Y. (2002) *Mol. Cell* 9, 1017–1029
108. Kundu, M., Guermah, M., Roeder, R. G., Amini, S., and Khalili, K. (1997) *J. Biol. Chem.* 272, 29468–29474
109. Phillips, A. C., Ernst, M. K., Bates, S., Rice, N. R., and Vousden, K. H. (1999) *Mol. Cell* 4, 771–781
110. Koki, A. T., and Masferrer, J. L. (2002) *Cancer Control* 9, Suppl. 2, 28–35
111. Soslow, R. A., Dannenberg, A. J., Rush, D., Woerner, B. M., Khan, K. N., Masferrer, J., and Koki, A. T. (2000) *Cancer* 89, 2637–2645
112. Yoshimura, R., Sano, H., Masuda, C., Kawamura, M., Tsubouchi, Y., Chargui, J., Yoshimura, N., Hla, T., and Wada, S. (2000) *Cancer* 89, 589–596
113. Shiota, G., Okubo, M., Noumi, T., Noguchi, N., Oyama, K., Takano, Y., Yashima, K., Kishimoto, Y., and Kawasaki, H. (1999) *Hepatogastroenterology* 46, 407–412
114. Kulkarni, S., Rader, J. S., Zhang, F., Liapis, H., Koki, A. T., Masferrer, J. L., Subbaramaiah, K., and Dannenberg, A. J. (2001) *Clin. Cancer Res.* 7, 429–434
115. Tucker, O. N., Dannenberg, A. J., Yang, E. K., Zhang, F., Teng, L., Daly, J. M., Soslow, R. A., Masferrer, J. L., Woerner, B. M., Koki, A. T., and Fahey, T. J., 3rd (1999) *Cancer Res.* 59, 987–990
116. Gately, S., and Li, W. W. (2004) *Semin. Oncol.* 31, 2–11
117. Dormond, O., Foletti, A., Paroz, C., and Ruegg, C. (2001) *Nat. Med.* 7, 1041–1047
118. Fosslien, E. (2001) *Ann. Clin. Lab. Sci.* 31, 325–348

FEBS 30091

FEBS Letters 579 (2005) 6279–6287

# ET-18-O-$CH_3$-induced apoptosis is causally linked to COX-2 upregulation in H-ras transformed human breast epithelial cells

Hye-Kyung Na[a], Hiroyasu Inoue[b], Young-Joon Surh[a,*]

[a] *National Research Laboratory of Molecular Carcinogenesis and Chemoprevention, College of Pharmacy, Seoul National University, Seoul 151-742, Republic of Korea*

[b] *South Korea and Department of Food Science and Nutrition, Nara Women's University, Nara, Japan*

Received 3 July 2005; accepted 10 September 2005

Available online 14 October 2005

Edited by Laszlo Nagy

**Abstract** Abnormally elevated expression of cyclooxygenase-2 (COX-2) has been frequently observed in transformed or malignant cells, and certain non-steroidal anti-inflammatory drugs with COX-2 inhibitory activity exert anti-neoplastic or chemopreventive effects. Contrary to this notion, we have found that a novel alkylphospholipid type antitumor agent ET-18-O-$CH_3$ (1-*O*-octadecyl-2-*O*-methyl-glycero-3-phosphocholine) induces COX-2 expression in H-*ras* transformed human breast epithelial cells (MCF10A-*ras*) while it causes apoptosis at the same concentration range. The addition of a selective COX-2 inhibitor SC-58635 and *COX-2* gene knock down with the siRNA blocked ET-18-O-$CH_3$-induced apoptosis, suggesting that COX-2 induction by this drug is causally linked to its apoptosis inducing activity. ET-18-O-$CH_3$ enhanced the transcriptional activities of cyclic AMP response element which is a key regulator of COX-2 expression. 15-Deoxy-$\Delta^{12,14}$ prostaglandin $J_2$ is, an endogenous ligand for peroxisome proliferator-activated receptor γ (PPARγ), has been known to possess proapoptotic potential in diverse cell types. ET-18-O-$CH_3$ treatment resulted in elevated release of 15d-$PGJ_2$ and DNA binding and transcriptional activity of PPARγ. Based on these findings, it is likely that ET-18-O-$CH_3$ induces COX-2 expression and production of 15d-$PGJ_2$ which may mediate the ET-18-O-$CH_3$-induced apoptosis in MCF10A-*ras* cells.


*Keywords:* Cyclooxygenase-2; Apoptosis; ET-18-O-$CH_3$; 15-Deoxy-$\Delta^{12,14}$-prostaglandin $J_2$; Human breast epithelial cells transformed with H-*ras* (MCF10A-*ras*)

## 1. Introduction

Cyclooxygenase (COX) initiates the conversion of arachidonate to a series of prostaglandins (PGs) and thromboxanes. Two isoforms of COX, i.e., COX-1 and COX-2, have been identified. COX-1, which is constitutively expressed in almost all tissues, is important for the maintenance of homeostatic functions, whereas COX-2, as an inducible isozyme, is transiently upregulated by pro-inflammatory cytokines, growth factors, tumor promoters, etc. [1]. Abnormal upregulation of COX-2 has been implicated in the pathogenesis of various human malignancies. There has been substantial body of data suggesting that COX-2 overexpression provides tumor cells with survival advantage leading to resistance to apoptosis and increased invasiveness or angiogenesis [2–4]. Conversely, selective COX-2 inhibitors have been shown to exert anti-carcinogenic activity [5,6]. Therefore, inhibition of COX-2 has been recognized as one of the most promising strategies for cancer prevention or treatment.

However, induction of COX-2 does not necessarily contribute to the cell survival or tolerance to proapoptotic insult. Thus, certain anticancer agents with pro-apoptotic activity were found to upregulate COX-2 expression in human hepatic myofibroblasts cells [7] and neuroglioma cells [8]. According to these studies, COX-2 inhibition by non-steroidal anti-inflammatory drugs (NSAID) blunted the anti-proliferative effect of these compound, suggesting that COX-2-derived PGs may be implicated in sensitizing these cells to apoptotic death. Moreover, in line with a possible proapoptotic function of COX-2, a major COX-2 product prostaglandin $E_2$ ($PGE_2$) [8] as well as 15-deoxy-$\Delta^{12,14}$-$PGJ_2$ (15d-$PGJ_2$) [9–11], a ligand of peroxisome proliferator-activated receptor γ (PPARγ), induced apoptosis in several types of cancer cells. Nonetheless, the molecular mechanism linking upregulation of COX-2 to induction of apoptosis has not been resolved yet.

ET-18-O-$CH_3$ (edelfosine; 1-*O*-octadecyl-2-*O*-methyl-*rac*-glycero-3-phosphocholine) is a synthetic analogue of 2-lysophosphatidylcholine that has been found to target cellular membranes and to exert potent anti-neoplastic effects [12,13]. ET-18-O-$CH_3$ has a broad spectrum of anti-tumorigenic effects [14–17]. The compound has been known to be a potent inducer of apoptosis in tumor cells, especially in leukemic cells, while sparing normal cells [18–20]. Inhibition of protein kinase C, phospholipase C, phosphatidylinositol 3-kinase, CTP: phosphocholine cytidylyltransferase, and coenzyme A-independent transacylase as well as blocking of arachidonate-phospholipid remodeling contributes to ET-18-O-$CH_3$-induced apoptosis [20–27]. ET-18-O-$CH_3$-induced apoptosis was accompanied by disruption of the mitochondrial transmembrane potential and activation of caspase-3 [15,28]. It also induces cell death by intracellular activation of the death receptor Fas/CD95 [18,29,30].

Here, we report that upregulation of COX-2 contributes to apoptotic death of the *ras*-transformed human mammary epithelial cells treated with the anti-cancer drug ET-18-O-$CH_3$.

## 2. Materials and methods

### 2.1. Materials

ET-18-O-$CH_3$ was purchased from BIOMOL Research Laboratories, Inc. (Plymouth Meeting, PA, USA). SC58635, a specific COX-2 inhibitor, was kindly provided by Pharmacia Korea. $PGE_2$ and

*Corresponding author. Fax: +82 2 874 9775.
*E-mail address:* surh@plaza.snu.ac.kr (Y.-J. Surh).

0014-5793/$30.00 
doi:10.1016/j.febslet.2005.09.094

15d-$PGJ_2$ were obtained from Cayman Chemicals (Ann Arbor, MI, USA). Dulbecco's modified Eagle's medium (DMEM)/F-12, heat-inactivated horse serum, L-glutamine, and penicillin/streptomycin/fungizone mixture were products of Gibco-BRL (Grand Island, NY, USA). Insulin, cholera toxin, hydrocortisone, recombinant epidermal growth factor, and actin antibody were purchased from the Sigma Chemical Co. (St. Louis, MO, USA). Antibodies against poly(ADP-ribose)polymerase (PARP) and COX-2 were from Santa Cruz Biotechnology (Santa Cruz, CA, USA). Cleaved PARP antibody was purchased from Cell Signaling Technology (Beverly, MA, USA). Secondary antibodies were obtained from Zymed Laboratories Inc. (San Francisco, CA, USA). The ECL chemiluminescent detection reagent was purchased from Amersham Co. (Arlington Heights, IL, USA). A series of human COX-2 promoter deletion constructs ligated to luciferase gene were described previously [31]. The putative peroxisome-proliferator reactive element (PPRE) firefly luciferase reporter construct (pPPRE-Luc) was kindly provided by Dr. Kang-Yell Choi (Yonsei University, Seoul, Korea). [$\gamma$-$^{32}$P]ATP was the product of NEN Life Science (Boston, MA, USA). ET-18-O-$CH_3$ was dissolved in 50% ethanol. Other substances were dissolved in DMSO and was further diluted with culture medium.

### 2.2. Cell culture

The MCF10A cell line transfected with a virus carrying the H-*ras* oncogene (MCF10A-*ras*) was cultured as described previously [32]. The cells were cultured in DMEM/F-12 medium supplemented with 5% heat-inactivated horse serum, 10 μg/ml insulin, 100 ng/ml cholera toxin, 0.5 μg/ml hydrocortisone, 20 ng/ml recombinant EGF, 2 mM L-glutamine, and 100 μg/ml penicillin/streptomycin/fungi zone mixture at 37 °C in a 5% $CO_2$ atmosphere.

### 2.3. Cell growth assay

MCF10A-*ras* cells at 50–60% confluence were inoculated into the plate and exposed to the medium containing chemicals. The cell viability was determined by the trypan blue exclusion method or the conventional MTT reduction assay as described previously [16,33]. All samples were prepared in triplicates.

### 2.4. Measurement of PGs

MCF10A-*ras* cells cultured in 6-well plates were treated with ET-18-O-$CH_3$ with or without SC58635 for 3 days. The amounts of $PGE_2$ released into media were measured using the enzyme-immunoassay kit (Amersham Biosciences Corp., NJ, USA) according to the manufacturer's instructions. Briefly, 50 μl of culture medium previously centrifuged at 200 × *g* for 10 min was mixed with 50 μl $PGE_2$ antibody solution in the plate coated with goat anti-mouse IgG followed by incubation on ice for 3 h. After 50 μl horseradish peroxidase conjugate $PGE_2$ was added to the reaction mixture, the plate was kept on ice for additional 1 h. After aspiration and rinse four times with washing buffer, 150 μl of 3,3′,5,5′-tetramethylbenzidine substrate solution was added and incubation was continued for 30 min at room temperature in a dark place. The reaction was terminated by addition of 100 μl of 1 M sulfuric acid, and the absorbance at 450 nm was read by the ELISA reader. $PGE_2$ was quantitated using a standard curve constructed with known concentrations of $PGE_2$. Likewise, 15d-$PGJ_2$ was assayed using an enzyme immunoassay kit (Assay Designs Inc., Ann Arbor, MI, USA).

### 2.5. In situ nick end-labeling (TUNEL)

To detect apoptosis at a single cell level, enzymatic in situ nick end-labeling (TUNEL) was carried out with an in situ death detection kit (Boehringer Mannheim, Mannheim, Germany), according to a manufacture's protocol. Briefly, MCF10A-*ras* cells were cultured in a chamber slide™ in the absence or presence of ET-18-O-$CH_3$ for 3 days. The cells were fixed for 30 min in 10% neutral-buffered formalin solution at room temperature. Endogenous peroxidase was inactivated by incubation with 0.3% (v/v) hydrogen peroxide in methanol for 1 h at room temperature and further incubated in a permeabilizing solution (0.1% sodium citrate and 0.1% Triton X-100) for 2 min at 4 °C. The cells were labeled by incubation with the TUNEL reaction mixture for 60 min at 37 °C followed by labeling with peroxidase-conjugated anti-fluorescein anti-goat antibody (Fab fragment) for additional 30 min. After being stained with diaminobenzidine for 10 min, cells were rinsed with phosphate-buffered saline (PBS) and mounted with 50% glycerol.

### 2.6. Measurement of sub-diploid DNA

MCF10A-*ras* cells plated at a density of $2 \times 10^5$ cells in 6-well plates were treated with ET-18-O-$CH_3$ in the presence or absence of SC58635 for 24 h. The cells were washed, trypsinized, collected by centrifuged at 200 × *g* for 5 min, fixed with 1 ml of 70% cold ethanol and stored at −20 °C until use. After centrifugation at 1300 × *g* for 10 min, the fixed cells were stained with PBS containing 0.1% Triton X-100, 0.1 mM EDTA (pH 7.4), 10 μg/ml RNase A, and 50 μg/ml PI, and 10 000 cells per sample were analyzed by a FACScalibur instrument (Backton–Dicknson, USA). The DNA histograms were further analyzed by CellQuest Pro software to calculate the proportion of sub-diploid cell population.

### 2.7. Measurement of mitochondrial transmembrane potential

To measure the mitochondrial transmembrane potential ($\Delta\psi_m$), the lipophilic cationic probe TMRE was used. MCF10A-*ras* cells were cultured in 4 chamber slide glasses (Nunc, IL, USA). After treatment, the cells were rinsed with PBS and incubated with TMRE (150 nM) in the fresh media for 30 min at 37 °C. The cells were examined under a confocal microscope (Leica Microsystems Heidelberg GmbH, Heidelberg, Germany) with the fluorescence excitation at 488 nm and emission at 590 nm.

### 2.8. Western blot analysis

Treated MCF10A-*ras* cells were washed with PBS and harvested after digestion with lysis buffer (150 mM NaCl, 0.5% Triton X-100, 50 mM Tris–HCl, pH 7.4, 25 mM NaF, 20 mM EGTA, 1 mM DTT, 1 mM $Na_3VO_4$, protease inhibitor cocktail tablet). Cellular debris was removed by centrifugation at 23 000 × *g* for 15 min at 4 °C. The protein concentration was determined by using the BCA protein assay kit (Pierce Biotechnology, Inc., Rockford, IL). After addition of sample loading buffer, proteins were electrophoresed on a 12.5% SDS–polyacrylamide gel. The proteins were transferred to polyvinylidene difluoride membranes at 300 mA for 3 h. The membranes were blocked in 5% dried milk reconstituted in 0.1% Tween 20 in PBS (PBST). The blots were then incubated with primary antibodies (COX-2, PPARγ, caspase-3) in 3% dried milk/PBST. The blots were washed three times with PBST, and incubated with horseradish peroxidase-conjugated secondary antibodies in 3% dried milk/PBST for 1 h. The blots were washed again three times with PBST, and immunoreactive protein complexes were detected by the ECL detection reagent according to the manufacturer's instructions and visualized with X-ray film.

### 2.9. Reverse-transcriptase polymerase chain reaction (RT-PCR)

Total RNA was isolated from MCF10A-*ras* cells using TRIzol® (Invitrogen, Carlsbad, CA, USA). One μg of total RNA was reverse-transcribed with murine leukemia virus reverse transcriptase (Promega, Madison, WI, USA) at 42 °C for 50 min and 72 °C for 15 min. The cycling conditions were as follows: 3 min at 95 °C followed by 35 cycles of 95 °C, 30 s; 63 °C, 1 min; 72 °C, 1 min of COX-2; 26 cycles of 94 °C, 1 min; 63 °C, 2 min; 72 °C, 2 min of the house keeping gene, glyceraldehyde-3-phosphate dehydrogenase (GAPDH) followed by a final extension at 72 °C for 10 min. The primer pairs (forward and reverse, respectively) and the size of the expected products were as follows: COX-2, 5′-CGGGATCCATGCTCGCCCGCGCCCTGCTGC-3′ and 5′-GCTCTAGAGCCTACAGTTCAGTCGAACGTTC-3′, 1800 base pair; GAPDH, 5′-TGAAGGTCGGTGTCAACGGATTTGGC-3′ and 5′-CATGTAGGCCATGAGGTCCACCAC-3′, 983 base pair. Amplification products were analyzed on 1.2% agarose gel electrophoresis, stained with ethidium bromide, and photographed under ultraviolet light.

### 2.10. Transient transfection and the luciferase assay

MCF10A-*ras* cells seeded at a density of $2 \times 10^5$/well in a 6-well dish were grown to 60–70% confluence in complete growth media. The cells were co-transfected with 2 μg of plasmid DNA constructs and 0.5 μg of pCMV-β galactosidase control vector with DOTAP liposomal transfection reagent (Roche Applied Science, Mannheim, Germany) according to the manufacturer's instructions. After 12-h transfection, the cells were treated with ET-18-O-$CH_3$ for additional 6 h and then washed

with PBS and lysed in 1× reporter lysis buffer (Promega, Madison, WI). The activities of firefly luciferase in the cell lysates were measured using the luciferase reporter assay system according to the manufacturer's instructions (Promega, Madison, WI) by Luminoskan luminometer (Thermo Labsystems, Helsinki, Finland). β-Galactosidase activity was measured by using the commercially available assay kit (Promega, Madison, WI). The relative luciferase activity was obtained by normalizing the firefly luciferase activity against the β-galactosidase activity.

*2.11. COX-2 siRNA transfection*

An oligonucleotide sequence for COX-2 siRNA was selected to knock down COX-2 expression by utilizing the siRNA Target Finder software at www.invitrogen.com. The human COX-2 specific siRNA (5′-AAG GGC UCU AGU AUA AUA GGA GAG G-3′) and the non-specific siRNA (5′-AAG AGG GCU CGA UUA UUA AGG AGG G-3′) were provided by Invitrogen (Carlsbad, CA, USA). MCF10A-*ras* cells were transfected with an oligonucleotide sequence for COX-2 siRNA or non-specific siRNA for 24 h with DOTAP liposomal transfection reagent (Roche Applied Science, Mannheim, Germany) according to the manufacturer's instructions. After 24 h transfection, the cells were treated with ET-18-O-$CH_3$ or vehicle alone for 6 h.

*2.12. Preparation of nuclear extracts*

MCF10A-*ras* cells were cultured in 100-mm dishes in the absence or presence of ET-18-O-$CH_3$. Cells were gently washed with cold PBS, scraped, and centrifuged at 1300 × *g* for 5 min. Pellets were suspended in cold hypotonic buffer [10 mM HEPES, pH 7.9, 1.5 mM $MgCl_2$, 0.3 mM EDTA, 0.1 mM phenylmethylsulfonylfluoride (PMSF)]. The lysates were incubated for 10 min on ice and then centrifuged at 20 200 × *g* for 15 min at 4 °C. The pellets were washed with hypotonic buffer and resuspended in hypertonic buffer (30 mM HEPES, 1.5 mM $MgCl_2$, 0.3 mM EDTA, 10% glycerol, 450 mM NaCl, 0.1 mM PMSF) in ice for 30 min during rocking followed by centrifugation at 20 200 × *g* for 15 min. After determination of the protein concentration, the supernatant was stored at −80 °C before use.

*2.13. Electrophoretic mobility shifty assay*

The oligonucleotides harboring the PPRE consensus sequence (5′-CCAAGGTCAAAGGT-3′) were end-labeled with [γ-$^{32}$P] ATP using T4 polynucleotide kinase (Takara, Japan). The nuclear protein (7–10 μg) was incubated with 8.5 μl of incubation buffer (30 mM HEPES, pH 7.9, 1.5 mM $MgCl_2$, 0.3 mM EDTA, pH 8.0, 10% glycerol), 2.5 μl polydI-dC (0.5 μg/μl), and the hypertonic buffer was added up to 20 μl of total volume. The reaction mixture was preincubated at room temperature for 15 min. The labeled oligonucleotide (50 000–100 000 cpm) was added and incubated for 30 min at room temperature for DNA-binding reactions. To ensure the specificity of the binding, a competition experiment was carried out by adding the excess unlabeled oligonucleotide to the reaction mixture before addition of the labeled oligonucleotide. Samples were separated on the 6% acrylamide gels at 150 mA in 0.25× tris–borate–EDTA buffer. After vacuum-dried, the gel was exposed to X-ray film for autoradiography at −70 °C.

## 3. Results

*3.1. ET-18-O-$CH_3$-induced apoptosis in MCF10A-ras cells*

Treatment of MCF10A-*ras* cells with ET-18-O-$CH_3$ inhibited the cell growth in a concentration dependent manner (Fig. 1A). ET-18-O-$CH_3$ treatment resulted in distinct morphological changes including rapid blebbing of plasma membrane and nuclear disintegration that are characteristic of apoptotic cell death (Fig. 1B). Moreover, MCF10A-*ras* cells treated with ET-18-O-$CH_3$ exhibited proteolytic cleavage of caspase-3 and the DNA repair enzyme PARP that are typical biochemical changes frequently observed in cells undergoing apoptotic death (Fig. 1C).

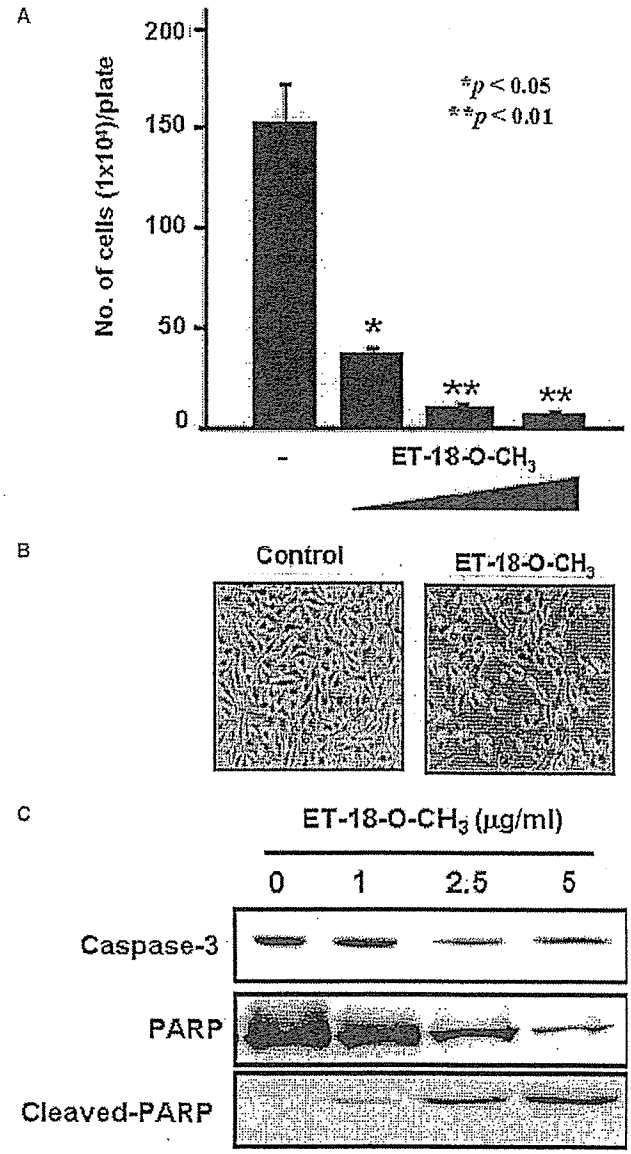


Fig. 1. Effects of ET-18-O-$CH_3$ on growth of MCF10A-*ras* cells. (A) The trypan blue dye exclusion method. Ten thousands of MCF10A-*ras* cells were inoculated into 35-mm dishes and exposed to the medium for 3 days with various concentrations (0, 1, 2.5, 5 μg/ml) of ET-18-O-$CH_3$. Treated cells were trypsinized followed by staining with trypan blue, and viable cells were counted by a hematocytometer. Bars represent means ± S.E.M. of triplicate experiments. A significant difference in the relative viability between treated cells and solvent controls is indicated with an asterisk. (B) Morphological changes in the MCF10A-*ras* cells treated with ET-18-O-$CH_3$ (2.5 μg/ml) for 1 day. Visualized by phase-contrast microscopy. (C) ET-18-O-$CH_3$-induced proteolytic cleavage of caspase-3 and PARP. MCF10A-*ras* cells were exposed to indicated concentrations of ET-18-O-$CH_3$ for 3 days. Protein from cell lysates was resolved by SDS–PAGE by Western blot using antibodies against caspase-3, PARP, and cleaved-PARP.

*3.2. ET-18-O-$CH_3$ upregulated COX-2 expression while inducing apoptosis*

Activated *ras* oncogene has been associated with upregulation of COX-2 in breast cancer cells [34], colorectal adenomas [35,36] and non-small cell lung cancer [37]. In recognition of this notion, we attempted to determine whether ET-18-O-$CH_3$ could induce apoptosis through downregulation of

COX-2 expression. Contrary to our expectation, ET-18-O-$CH_3$-induced COX-2 expression at both protein and mRNA levels in a concentration dependent manner, whereas basal COX-2 expression in MCF10A-*ras* cells remained relatively low (Fig. 2A and B). Unlike COX-2, the expression of COX-1 was not affected by ET-18-O-$CH_3$ treatment in MCF10A-*ras* cells (data not shown). In parallel with elevated COX-2 expression, $PGE_2$ production was also significantly increased upon ET-18-O-$CH_3$ treatment (Fig. 2C).

### 3.3. Upregulation of COX-2 was causally linked to ET-18-O-$CH_3$-induced apoptosis in MCF10A-ras cells

Although upregulation of COX-2 expression has been frequently associated with resistance to apoptosis, ET-18-O-$CH_3$-induced apoptosis and COX-2 expression in MCF10A-*ras* cells under the same experiment conditions. To examine whether ET-18-O-$CH_3$-induced COX-2 expression contributes to induction of apoptosis, a selective COX-2 inhibitor SC58635 was utilized. SC58635 inhibited ET-18-O-$CH_3$-induced production of $PGE_2$ in MCF10A-*ras* cells (Fig. 3A). We observed that SC58635, at a concentration that blocks COX-2, protected MCF10A-*ras* from ET-18-O-$CH_3$-induced proteolytic cleavage of caspase-3 (Fig. 3B). The same concentration of SC58635 inhibited the ET-18-O-$CH_3$-induced DNA fragmentation and lowered the sub $G_0/G_1$ proportion as measured by TUNEL staining and flow cytometry, respectively (Fig. 3C). The pharmacologic inhibition of COX-2 also restored the mitochondrial transmembrane potential ($\Delta\psi_m$) which was perturbed in ET-18-O-$CH_3$ treated cells (Fig. 3C). Likewise, the ET-18-O-$CH_3$-induced PARP cleavage was abolished upon direct *COX-2* gene knock down by employing the COX-2 siRNA (Fig. 3D), lending further support to the notion that upregulation of COX-2 expression is causally linked to induction of apoptosis in MCF10A-*ras* cells.

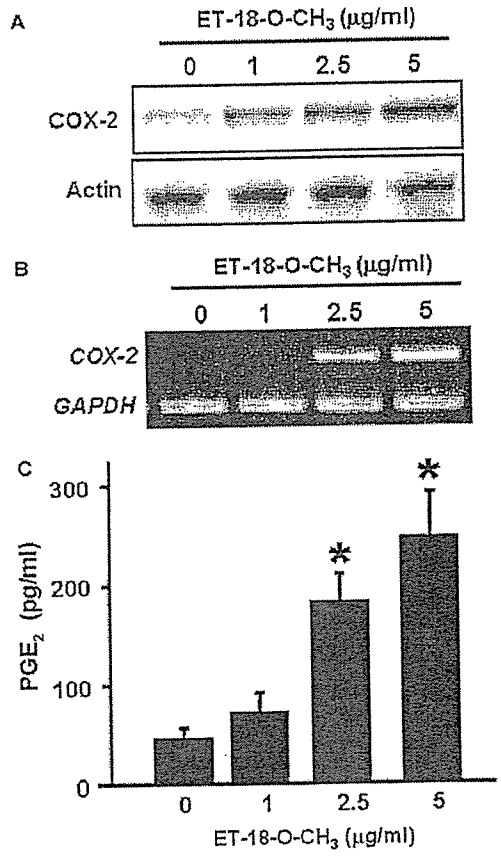


Fig. 2. Effects of ET-18-O-$CH_3$ on expression of COX-2 and $PGE_2$ production in MCF10A-*ras* cells. (A) Western blot analysis of COX-2 protein expression. MCF10A-*ras* cells were treated with various concentrations of ET-18-O-$CH_3$ for 3 days. Protein extracts from the cells were immunoblotted with anti-COX-2 antibody. (B) Determination of the relative amount of *COX-2* mRNA. Total RNA was extracted with TRIzol®, and RT-PCR for COX-2 mRNA transcripts was carried out as described under Section 2.9. GAPDH was used as an equal loading control. (C) ET-18-O-$CH_3$-induced $PGE_2$ production in MCF10A-*ras* cells. $PGE_2$ production was measured 3 days later by using the $PGE_2$ enzyme immunoassay kit following the manufacturer's protocol. A significant difference between treated cells and solvent controls is indicated with an asterisk ($P < 0.01$).

### 3.4. ET-18-O-$CH_3$ enhanced the COX-2 promoter activity

The regulation of COX-2 synthesis occurs mainly at the transcriptional level, although mRNA stabilization is also involved in response to specific signals. The types and nature of stimuli, signal transduction pathways, and transcription factors involved in the induction of *COX-2* gene expression are extremely diversified and cell specific. Several *cis*-acting elements are found in the COX-2 promoter, such as nuclear factor-κB (NF-κB), nuclear factor-interleukin-6 (NF-IL6), cyclic AMP response element (CRE), and E-box [38,39]. In order to determine which transcription factors are involved in ET-18-O-$CH_3$-induced COX-2 expression, MCF10A-*ras* cells were transiently transfected with human COX-2 promoter luciferase constructs (−1432/+59) (Fig. 4A) and challenged with ET-18-O-$CH_3$ for 6 h. Treatment with ET-18-O-$CH_3$ resulted in about a 6-fold increase in the *COX-2* promoter (−1432/+59) activity. To elucidate the critical region of the COX-2 promoter responsible for COX-2 expression by ET-18-O-$CH_3$, we utilized a series of *COX-2* deletion constructs (−1432/+59, −327/+59, −220/+59, −124/+59, and −52/+59). The *COX-2* promoter activity was most prominent when the −327/+59 promoter construct was used (Fig. 4B). As the promoter length was shortened, COX-2 activities were diminished gradually. It is noticeable that the −52/+59 construct exhibited an approximately 97% loss of the *COX-2* promoter activity compared with the −327/+59 construct. A CRE is present between nucleotides −59 and −53, suggesting that this element might responsible for mediating the COX-2 inducing effects of ET-18-O-$CH_3$. To precisely define which of these *cis*-acting elements are involved in ET-18-O-$CH_3$-induced *COX-2* promoter activity, MCF10A-*ras* cells were transiently transfected with site-specific mutant *COX-2* promoter constructs. As shown in Fig. 4C, CRM (−327/+59 construct in which mutated at the CRE site) significantly decreased the *COX-2* promoter activity in ET-18-O-$CH_3$-treated cells. The introduction of ILM (mutated at the NF-IL6 site) resulted in approximately 2-fold reduction, compared with the wild type −327/+59 construct while little effect on *COX-2* promoter activity was achieved with KBM (mutated at the NF-κB site) (Fig. 4C). These results suggest that CRE and possibly NF-IL6 play important role in mediating the induction of COX-2 gene expression.

### 3.5. ET-18-O-$CH_3$ induced production of 15d-$PGJ_2$ and expression as well as activation of PPARγ

To clarify how COX-2 upregulation by ET-18-O-$CH_3$ leads to induction of apoptosis in MCF10A-*ras* cells, we attempted

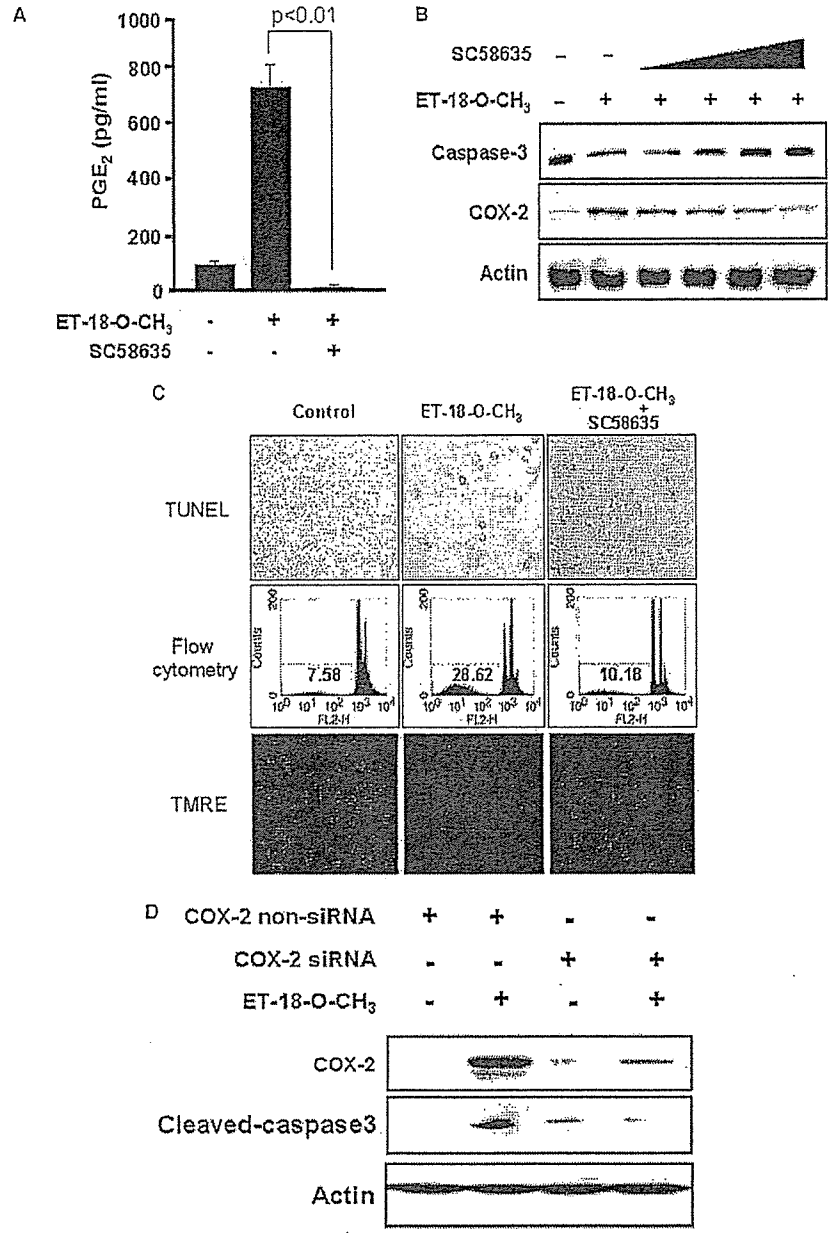


Fig. 3. Effects of the specific COX-2 inhibitor SC58635 on the ET-18-O-$CH_3$-induced apoptosis in MCF10A-*ras* cells. (A) Relative amount of $PGE_2$ released in the media following co-treatment of ET-18-O-$CH_3$ (2.5 μg/ml) for 3 days with SC58635 in the MCF10A-*ras* cells. (B) Effects of SC58635 on ET-18-O-$CH_3$-induced COX-2 expression as well as caspase-3 activation measured by Western blot analysis. MCF10A-*ras* cells were co-treated with ET-18-O-$CH_3$ (2.5 μg/ml) and 10, 25, 50 μM of SC58635 for 3 days. Protein extracts from the cells were immunoblotted with anti-COX-2, anti-caspase-3, and anti-actin antibodies. (C) SC58635 attenuation of ET-18-O-$CH_3$-induced apoptosis as determined by TUNEL, flow cytometry, and mitochondrial transmembrane permeability ($\Delta\psi_m$) changes. Cells were treated with ET-18-O-$CH_3$ (2.5 μg/ml) in the absence or presence of SC58635 (50 μM) for 1 day. (D) Effects of COX-2 siRNA on the ET-18-O-$CH_3$-induced COX-2 expression and cleaved PARP measured by Western blot analysis. MCF10A-*ras* cells were transfected with 20 nM non-specific and COX-2 specific siRNA before ET-18-O-$CH_3$ treatment.

to examine the products of COX-2. Among the COX-2-products, 15d-$PGJ_2$, an endogenous PPARγ ligand, has been known to possess pro-apoptotic potential in diverse cancer cells [40]. To examine whether 15d-$PGJ_2$ can mediate ET-18-O-$CH_3$-induced apoptosis, we measured the production of this cyclopentenone PG in the MCF10A-*ras* cells treated with ET-18-O-$CH_3$. 15d-$PGJ_2$ production was significantly elevated after treatment of ET-18-O-$CH_3$ (Fig. 5A). Again, SC58635 suppressed the production of 15d-$PGJ_2$ induced by ET-18-O-$CH_3$ (Fig. 5A). We also observed that exogenously added 15d-$PGJ_2$ inhibited the growth of MCF10A-*ras* cells (Fig. 5B) and induced apoptosis in MCF10A-*ras* cells as revealed by proteolytic cleavage of caspase-3 (Fig. 5C). As an endogenous ligand of PPARγ, 15d-$PGJ_2$ is likely to exert its biologic effects in part via PPARγ. Moreover, ET-18-O-$CH_3$ activated expression of PPARγ as well as COX-2 which preceded the activation of caspase-3 through proteolytic cleavage (Fig. 5D). We also observed that ET-18-O-$CH_3$ induced the

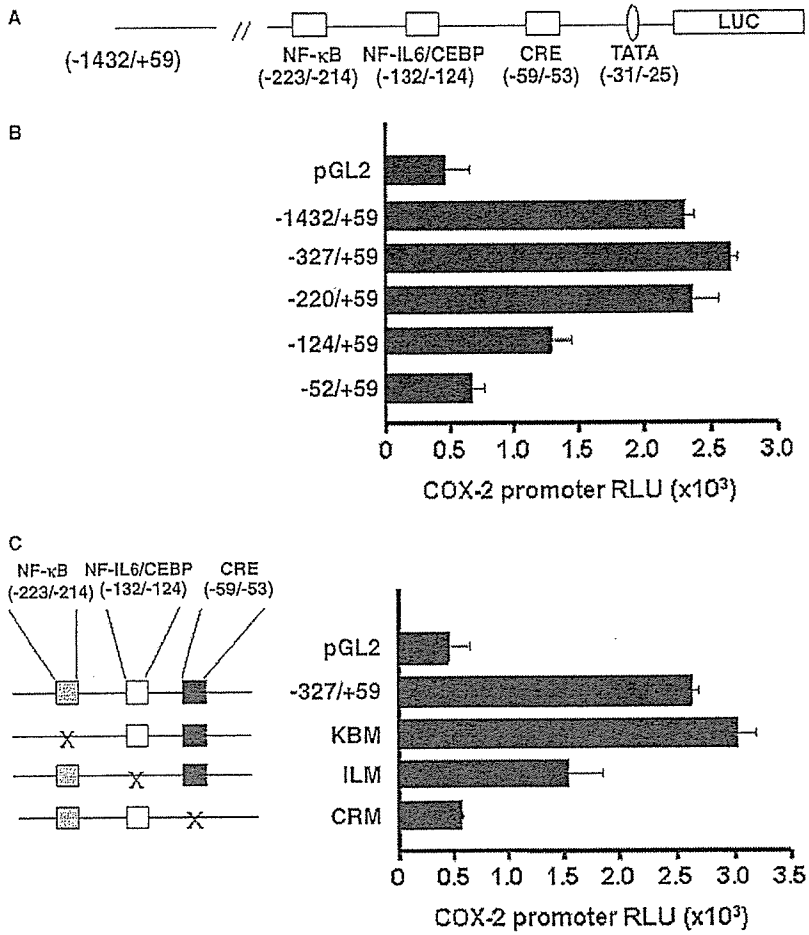


Fig. 4. ET-18-O-$CH_3$-induced activation of the COX-2 promoter. (A) A schematic representation of the human COX-2 promoter. (B) Determination of *cis*-acting elements of COX-2 promoter. MCF10A-*ras* cells were transfected with the 2.5 μg of a series of human COX-2 promoter deletion constructs (−1432/+59, −327/+59, −220/+59, −124/+59, −52/+59) ligated to luciferase. (C) Identification of the regions responsible for ET-18-O-$CH_3$-induced promoter activity of the human COX-2 gene. MCF10A-*ras* cells were transfected with 2.5 μg of a series of human COX-2 pormoter-luciferase constructs (−327/+59, KBM; ILM; CRM). KBM represents the −327/+59 COX-2 promoter construct in which the NF-κB site was mutated. ILM represents the −327/+59 COX-2 promoter construct in which the NF-IL6 site was mutated. CRM refers to the −327/+59 COX-2 promoter construct in which the CRE site was mutated. For the experiments related to B and C, MCF10A-*ras* cells were transiently co-transfected with pCOX-2 promoter and pCMV-β galactosidase (0.5 μg) for 24 h by using DOTAP Liposomal Transfection Reagent according to the manufacturer's instructions. Transfectant cells were treated with ET-18-O-$CH_3$ (2.5 μg/ml) for 4 h and the cells were lysed with reporter lysis buffer for measurement of luciferase activity. Luciferase activity represents data that have been normalized to β-galactosidase activity.

PPRE binding activity (Fig. 5E) and transcriptional activity (Fig. 5F) of PPARγ in MCF10A-*ras* cells. Therefore, ET-18-O-$CH_3$-induced COX-2 expression and subsequent production of 15d-$PGJ_2$ are likely to contribute to induction of apoptosis in MCF10A-*ras* cells.

## 4. Discussion

Multiple lines of evidence indicate that aberrant overexpression of COX-2 is implicated in inhibition of apoptosis and induced proliferation [2]. Tumor formation and growth are reduced in animals that are either genetically engineered to be COX-2 deficient or treated with a pharmacologic inhibitor of COX-2 [41–43]. The use of NSAIDs has been associated with a reduced risk of several malignancies through inhibition of COX-2 activity [44,45]. Moreover intake of the selective COX-2 inhibitor celecoxib reduced the burden of colorectal polyps in patients with familial adenomatous polyposis and has been shown to inhibit experimentally induced carcinogenesis [6,46,47]. Inhibition of COX-2 is hence recognized as one of the most feasible strategies for cancer chemoprevention and treatment.

Contrary to these findings, our present study clearly demonstrates that upregulation of COX-2 is causally linked to ET-18-O-$CH_3$-induced apoptosis in MCF10A-*ras* cells as a selective COX-2 inhibitor blocked the ET-18-O-$CH_3$-induced cell death. In this study, we found that mutation of the CRE binding site completely abolished the COX-2 promoter activity, suggesting that this site located in the COX-2 promoter plays a crucial role in regulating COX-2 transcription. Knock-down of COX-2 expression by siRNA also attenuated apoptosis induced by ET-18-O-$CH_3$. Other investigators have also reported that some of agents upregulate COX-2 expression while inducing apoptosis [7,48]. Thus, sphingosin 1-phosphate, a bioactive sphingolipid with growth-regulating properties,

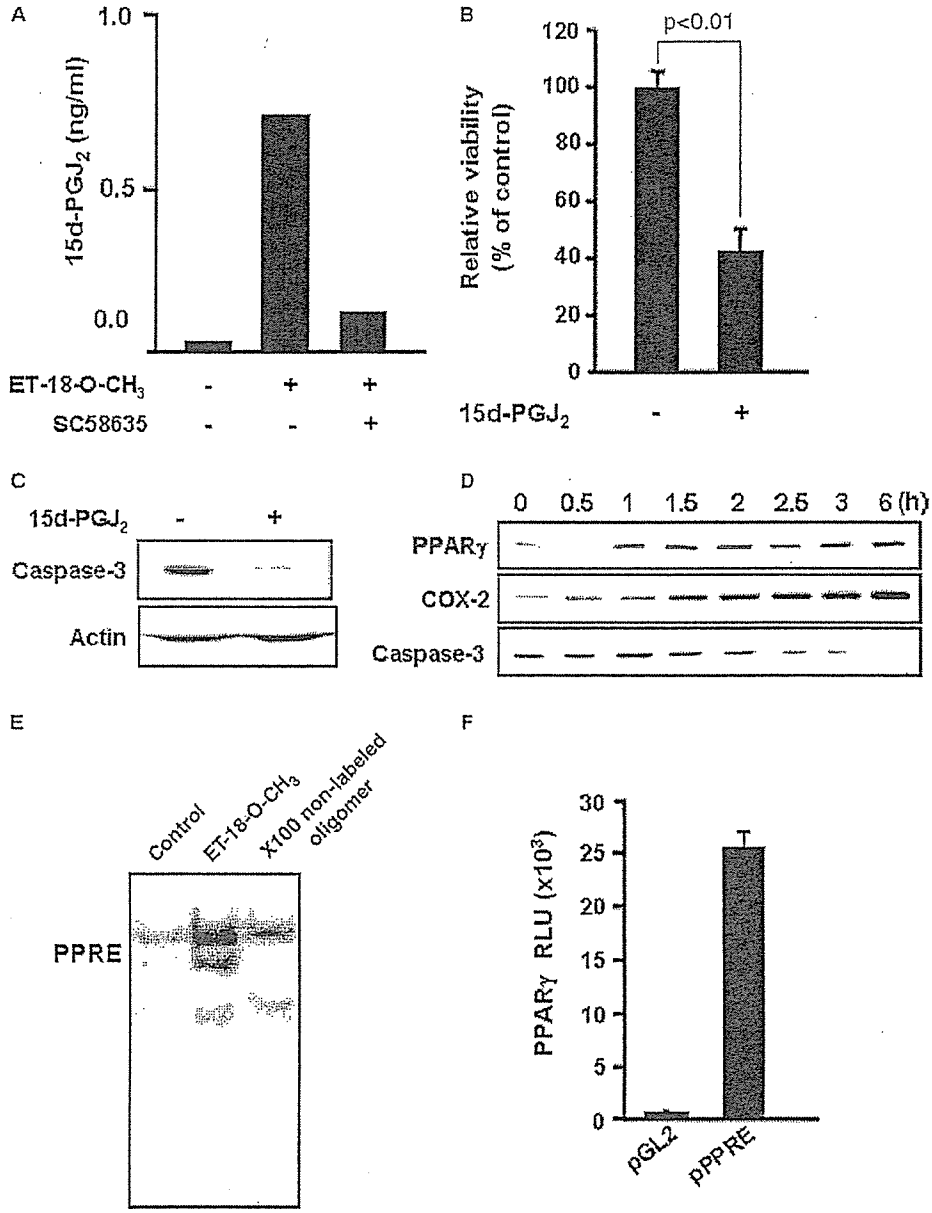


Fig. 5. Possible involvement of 15-$PGJ_2$ production in ET-18-O-$CH_3$-induced apoptosis. (A) Production of 15d-$PGJ_2$ in ET-18-O-$CH_3$ treated MCF10A-*ras* cells. The amounts of 15d-$PGJ_2$ released into media were measured after treatment of the cells with 2.5 μg/ml of ET-18-O-$CH_3$ for 1 days. (B) 15d-$PGJ_2$ induced anti-proliferative effect in MCF10A-*ras* cells. Cell viability was measured by the conventional MTT reduction assay after treatment with 15d-$PGJ_2$ (10 μM) for 1 day. Bars represent means ± S.E.M. of triplicate experiments. (C) 15d-$PGJ_2$ induced apoptosis in MCF10A-*ras* cells as evidenced by caspase-3 cleavage. (D) ET-18-O-$CH_3$ induced expression of PPARγ, COX-2, and caspase-3 cleavage as determined by immunoblot analysis. The concentration of ET-18-O-$CH_3$ was 2.5 μg/ml. (E) DNA-binding activity of PPARγ in ET-18-O-$CH_3$ treatment MCF10A-*ras* cells. Nuclear extracts were prepared from MCF10A-*ras* cells treated with ET-18-O-$CH_3$ for 30 min and incubated with the [$\gamma$-$P^{32}$] labeled oligonucleotide harboring PPRE, followed by electrophoretic mobility shifty assay. (F) Relative luciferase activity representing the transcriptional activity of PPARγ. MCF10A-*ras* cells were transiently co-transfected with pPPRE-Luc and pCMV-β galactosidase for 24 h using DOTAP Liposomal Transfection Reagent according to the manufacturer's instructions. Transfectant cells were treated with ET-18-O-$CH_3$ (2.5 μg/ml) for 6 h and the cells were lysed with reporter lysis buffer for the measurement of luciferase activity.

induced COX-2 expression and apoptosis, and blocking COX-2 by NS-398 blunted the anti-proliferative effect of sphingosin 1-phosphate in human hepatic myofibroblasts cells [7]. More recently, *R*(+)-methanandamide-induced cell death has been found to be associated with COX-2 upregulation in human neuroglioma cells [8]. Some of PGs are known to have proapoptotic activity. For instance, 15d-$PGJ_2$, a potent natural ligand for PPARγ, induces apoptosis in several types of cancer cells [49,50]. When MCF10A-*ras* cells were treated with exogenously added 15d-$PGJ_2$, this cyclopentenone PG induced apoptosis in MCF10A-*ras* cells. Moreover, ET-18-O-$CH_3$ treatment augmented production of 15d-$PGJ_2$. Biological effects of 15d-$PGJ_2$ could be elicited via several distinct mechanisms, either PPARγ-dependent or -independent. We found that ET-18-O-$CH_3$ induced expression of PPARγ and its subsequent binding to PPRE and transcriptional activity. It has

been reported that PPRE is located in the 5′ flanking region of the COX-2 promoter, and that induction of COX-2 expression by NSAIDs and PPARγ ligands is mediated via this element [51].

Besides COX-2-dependent induction of apoptosis we demonstrated in the present work, there might be other mechanisms which can also be attributable to ET-18-O-$CH_3$-induced apoptosis in MCF10A-*ras* cells. In this context, it is interesting to note that ET-18-O-$CH_3$-induced apoptosis is associated with production of reactive oxygen species in p53-defective hepatocytes [15] and HL-60 cells [28].

Blockade of ET-18-O-$CH_3$-induced apoptosis by SC58635 may have clinical implications. Recently, the chemotherapeutic agent paclitaxel-induced apoptosis in ovarian cancer cells, but combining treatment with COX-2 inhibitors resulted in a significant inhibition of paclitaxel-induced apoptosis, suggesting that combination of COX-2 inhibitors with chemotheraphy agents does not have an additive or synergistic tumoricidal effect [52]. If the same effect is true in vivo, the use of COX inhibitors prior to or concurrent with anticancer drug might carry a negative effect on therapeutic efficacy. Although COX-2 selective inhibitors are obviously have chemopreventive potential, it is necessary to examine carefully any adverse effects at the whole body level before considering their application for clinical.

In summary, COX-2 upregulation contributes to induction of apoptosis in MCF10A-*ras* cells treated with the anti-cancer drug ET-18-O-$CH_3$. These findings suggest that inhibition of COX-2 expression is not necessarily desirable for cancer prevention or therapy. It seems likely that the physiological functions of COX-2 depend on the types of inducers and cells, and targeted inhibition of COX-2 in the context of anticancer therapy may need more through validation.

*Acknowledgment:* This work was supported by Grant R02-2004-000-10197-0 from the Basic Research Program of the Korea Research Foundation (to Y.-J. Surh).

## References

[1] DuBois, R.N., Awad, J., Morrow, J., Roberts II, L.J. and Bishop, P.R. (1994) Regulation of eicosanoid production and mitogenesis in rat intestinal epithelial cells by transforming growth factor-α and phorbol ester. J. Clin. Invest. 93, 493–498.

[2] Ishiko, O., Sumi, T., Yoshida, H., Matsumoto, Y., Honda, K., Deguchi, M., Yamada, R. and Ogita, S. (2001) Association between overexpression of cyclooxygenase-2 and suppression of apoptosis in advanced cancer of the uterine cervix after cyclic balloon-occluded arterial infusion. Oncol. Rep. 8, 1259–1263.

[3] Mohammed, S.I., Knapp, D.W., Bostwick, D.G., Foster, R.S., Khan, K.N., Masferrer, J.L., Woerner, B.M., Snyder, P.W. and Koki, A.T. (1999) Expression of cyclooxygenase-2 (COX-2) in human invasive transitional cell carcinoma (TCC) of the urinary bladder. Cancer Res. 59, 5647–5650.

[4] Cianchi, F., Cortesini, C., Bechi, P., Fantappie, O., Messerini, L., Vannacci, A., Sardi, I., Baroni, G., Boddi, V., Mazzanti, R. and Masini, E. (2001) Up-regulation of cyclooxygenase 2 gene expression correlates with tumor angiogenesis in human colorectal cancer. Gastroenterology 121, 1339–1347.

[5] Chun, K.S. and Surh, Y.J. (2004) Signal transduction pathways regulating cyclooxygenase-2 expression: potential molecular targets for chemoprevention. Biochem. Pharmacol. 68, 1089–1100.

[6] Chun, K.S., Kim, S.H., Song, Y.S. and Surh, Y.J. (2004) Celecoxib inhibits phorbol ester-induced expression of COX-2 and activation of AP-1 and p38 MAP kinase in mouse skin. Carcinogenesis 25, 713–722.

[7] Davaille, J., Gallois, C., Habib, A., Li, L., Mallat, A., Tao, J., Levade, T. and Lotersztajn, S. (2000) Antiproliferative properties of sphingosine 1-phosphate in human hepatic myofibroblasts. A cyclooxygenase-2 mediated pathway. J. Biol. Chem. 275, 34628–34633.

[8] Hinz, B., Ramer, R., Eichele, K., Weinzierl, U. and Brune, K. (2004) Up-regulation of cyclooxygenase-2 expression is involved in *R*(+)-methanandamide-induced apoptotic death of human neuroglioma cells. Mol. Pharmacol. 66, 1643–1651.

[9] Clay, C.E., Namen, A.M., Atsumi, G., Willingham, M.C., High, K.P., Kute, T.E., Trimboli, A.J., Fonteh, A.N., Dawson, P.A. and Chilton, F.H. (1999) Influence of J series prostaglandins on apoptosis and tumorigenesis of breast cancer cells. Carcinogenesis 20, 1905–1911.

[10] Li, L., Tao, J., Davaille, J., Feral, C., Mallat, A., Rieusset, J., Vidal, H. and Lotersztajn, S. (2001) 15-deoxy-Delta$^{12,14}$-prostaglandin $J_2$ induces apoptosis of human hepatic myofibroblasts. A pathway involving oxidative stress independently of peroxisome-proliferator-activated receptors. J. Biol. Chem. 276, 38152–38158.

[11] Shen, Z.N., Nishida, K., Doi, H., Oohashi, T., Hirohata, S., Ozaki, T., Yoshida, A., Ninomiya, Y. and Inoue, H. (2005) Suppression of chondrosarcoma cells by 15-deoxy-$\Delta^{12,14}$-prostaglandin $J_2$ is associated with altered expression of Bax/Bcl-xL and p21. Biochem. Biophys. Res. Commun. 328, 375–382.

[12] Berkovic, D. (1998) Cytotoxic etherphospholipid analogues. Gen. Pharmacol. 31, 511–517.

[13] Dimanche-Boitrel, M.T., Meurette, O., Rebillard, A. and Lacour, S. (2005) Role of early plasma membrane events in chemotherapy-induced cell death. Drug Resist. Updat. 8, 5–14.

[14] Slaton, J.W., Hampton, J.A. and Selman, S.H. (1994) Exposure to alkyllysophospholipids inhibits in vitro invasion of transitional cell carcinoma. J. Urol. 152, 1594–1598.

[15] Vrablic, A.S., Albright, C.D., Craciunescu, C.N., Salganik, R.I. and Zeisel, S.H. (2001) Altered mitochondrial function and overgeneration of reactive oxygen species precede the induction of apoptosis by 1-*O*-octadecyl-2-methyl-*rac*-glycero-3-phosphocholine in p53-defective hepatocytes. FASEB J. 15, 1739–1744.

[16] Na, H.K., Chang, C.C. and Trosko, J.E. (2003) Growth suppression of a tumorigenic rat liver cell line by the anticancer agent, ET-18-O-$CH_3$, is mediated by inhibition of cytokinesis. Cancer Chemother. Pharmacol. 51, 209–215.

[17] Candal, F.J., Bosse, D.C., Vogler, W.R. and Ades, E.W. (1994) Inhibition of induced angiogenesis in a human microvascular endothelial cell line by ET-18-$OCH_3$. Cancer Chemother. Pharmacol. 34, 175–178.

[18] Gajate, C., Fonteriz, R.I., Cabaner, C., Alvarez-Noves, G., Alvarez-Rodriguez, Y., Modolell, M. and Mollinedo, F. (2000) Intracellular triggering of Fas, independently of FasL, as a new mechanism of antitumor ether lipid-induced apoptosis. Int. J. Cancer 85, 674–682.

[19] Mollinedo, F., Martinez-Dalmau, R. and Modolell, M. (1993) Early and selective induction of apoptosis in human leukemic cells by the alkyl-lysophospholipid ET-18-$OCH_3$. Biochem. Biophys. Res. Commun. 192, 603–609.

[20] Shafer, S.H. and Williams, C.L. (2003) Non-small and small cell lung carcinoma cell lines exhibit cell type-specific sensitivity to edelfosine-induced cell death and different cell line-specific responses to edelfosine treatment. Int. J. Oncol. 23, 389–400.

[21] Civoli, F. and Daniel, L.W. (1998) Quaternary ammonium analogs of ether lipids inhibit the activation of protein kinase C and the growth of human leukemia cell lines. Cancer Chemother. Pharmacol. 42, 319–326.

[22] Powis, G., Seewald, M.J., Gratas, C., Melder, D., Riebow, J. and Modest, E.J. (1992) Selective inhibition of phosphatidylinositol phospholipase C by cytotoxic ether lipid analogues. Cancer Res. 52, 2835–2840.

[23] Ruiter, G.A., Verheij, M., Zerp, S.F. and van Blitterswijk, W.J. (2001) Alkyl-lysophospholipids as anticancer agents and enhancers of radiation-induced apoptosis. Int. J. Radiat. Oncol. Biol. Phys. 49, 415–419.

[24] Guo, H.B., Shen, Z.H., Huang, C.X., Ma, J., Huang, Y. and Chen, H.L. (2000) Modulation of the basal activity of phosphatidylinositol-3-kinase/protein kinase B signaling pathway in human hepatocarcinoma cells. Glycoconjugate J. 17, 315–322.

[25] Baburina, I. and Jackowski, S. (1998) Apoptosis triggered by 1-*O*-octadecyl-2-*O*-methyl-*rac*-glycero-3-phosphocholine is prevented by increased expression of CTP:phosphocholine cytidylyltransferase. J. Biol. Chem. 273, 2169–2173.
[26] Winkler, J.D., Eris, T., Sung, C.M., Chabot-Fletcher, M., Mayer, R.J., Surette, M.E. and Chilton, F.H. (1996) Inhibitors of coenzyme A-independent transacylase induce apoptosis in human HL-60 cells. J. Pharmacol. Exp. Ther. 279, 956–966.
[27] Surette, M.E., Winkler, J.D., Fonteh, A.N. and Chilton, F.H. (1996) Relationship between arachidonate–phospholipid remodeling and apoptosis. Biochemistry 35, 9187–9196.
[28] Gajate, C., Santos-Beneit, A.M., Macho, A., Lazaro, M., Hernandez-De Rojas, A., Modolell, M., Munoz, E. and Mollinedo, F. (2000) Involvement of mitochondria and caspase-3 in ET-18-$OCH_3$-induced apoptosis of human leukemic cells. Int. J. Cancer 86, 208–218.
[29] Mollinedo, F., Gajate, C., Martin-Santamaria, S. and Gago, F. (2004) ET-18-OCH3 (edelfosine): a selective antitumour lipid targeting apoptosis through intracellular activation of Fas/CD95 death receptor. Curr. Med. Chem. 11, 3163–3184.
[30] Gajate, C., Del Canto-Janez, E., Acuna, A.U., Amat-Guerri, F., Geijo, E., Santos-Beneit, A.M., Veldman, R.J. and Mollinedo, F. (2004) Intracellular triggering of Fas aggregation and recruitment of apoptotic molecules into Fas-enriched rafts in selective tumor cell apoptosis. J. Exp. Med. 200, 353–365.
[31] Inoue, H., Yokoyama, C., Hara, S., Tone, Y. and Tanabe, T. (1995) Transcriptional regulation of human prostaglandin-endoperoxide synthase-2 gene by lipopolysaccharide and phorbol ester in vascular endothelial cells. Involvement of both nuclear factor for interleukin-6 expression site and cAMP response element. J. Biol. Chem. 270, 24965–24971.
[32] Na, H.K. and Surh, Y.J. (2002) Induction of cyclooxygenase-2 in Ras-transformed human mammary epithelial cells undergoing apoptosis. Ann. N.Y. Acad. Sci. 973, 153–160.
[33] Chen, Z.H., Na, H.K., Hurh, Y.J. and Surh, Y.J. (2005) 4-Hydroxyestradiol induces oxidative stress and apoptosis in human mammary epithelial cells: possible protection by NF-κB and ERK/MAPK. Toxicol. Appl. Pharmacol. 208, 46–56.
[34] Gilhooly, E.M. and Rose, D.P. (1999) The association between a mutated ras gene and cyclooxygenase-2 expression in human breast cancer cell lines. Int. J. Oncol. 15, 267–270.
[35] Fujita, M., Fukui, H., Kusaka, T., Morita, K., Fujii, S., Ueda, Y., Chiba, T., Sakamoto, C., Kawamata, H. and Fujimori, T. (2000) Relationship between cyclooxygenase-2 expression and K-*ras* gene mutation in colorectal adenomas. J. Gastroenterol. Hepatol. 15, 1277–1281.
[36] Bissonnette, M., Khare, S., von Lintig, F.C., Wali, R.K., Nguyen, L., Zhang, Y., Hart, J., Skarosi, S., Varki, N., Boss, G.R. and Brasitus, T.A. (2000) Mutational and nonmutational activation of p21ras in rat colonic azoxymethane-induced tumors: effects on mitogen-activated protein kinase, cyclooxygenase-2, and cyclin D1. Cancer Res. 60, 4602–4609.
[37] Heasley, L.E., Thaler, S., Nicks, M., Price, B., Skorecki, K. and Nemenoff, R.A. (1997) Induction of cytosolic phospholipase A2 by oncogenic Ras in human non-small cell lung cancer. J. Biol. Chem. 272, 14501–14504.
[38] Howe, L.R., Subbaramaiah, K., Brown, A.M. and Dannenberg, A.J. (2001) Cyclooxygenase-2: a target for the prevention and treatment of breast cancer. Endocr. Relat. Cancer 8, 97–114.
[39] Inoue, H., Umesono, K., Nishimori, T., Hirata, Y. and Tanabe, T. (1999) Glucocorticoid-mediated suppression of the promoter activity of the cyclooxygenase-2 gene is modulated by expression of its receptor in vascular endothelial cells. Biochem. Biophys. Res. Commun. 254, 292–298.
[40] Na, H.K. and Surh, Y.J. (2003) Peroxisome proliferator-activated receptor γ (PPARγ) ligands as bifunctional regulators of cell proliferation. Biochem. Pharmacol. 66, 1381–1391.
[41] Oshima, M., Murai, N., Kargman, S., Arguello, M., Luk, P., Kwong, E., Taketo, M.M. and Evans, J.F. (2001) Chemoprevention of intestinal polyposis in the $Apc^{\Delta 716}$ mouse by rofecoxib, a specific cyclooxygenase-2 inhibitor. Cancer Res. 61, 1733–1740.
[42] Rao, C.V., Rivenson, A., Simi, B., Zang, E., Kelloff, G., Steele, V. and Reddy, B.S. (1995) Chemoprevention of colon carcinogenesis by sulindac, a nonsteroidal anti-inflammatory agent. Cancer Res. 55, 1464–1472.
[43] Oshima, H., Oshima, M., Inaba, K. and Taketo, M.M. (2004) Hyperplastic gastric tumors induced by activated macrophages in COX-2/mPGES-1 transgenic mice. EMBO J. 23, 1669–1678.
[44] Harris, R.E., Beebe-Donk, J. and Schuller, H.M. (2002) Chemoprevention of lung cancer by non-steroidal anti-inflammatory drugs among cigarette smokers. Oncol. Rep. 9, 693–695.
[45] Stockbrugger, R.W. (1999) Nonsteroidal anti-inflammatory drugs (NSAIDs) in the prevention of colorectal cancer. Eur. J. Cancer Prev. 8 (Suppl. 1), S21–S25.
[46] Phillips, R.K., Wallace, M.H., Lynch, P.M., Hawk, E., Gordon, G.B., Saunders, B.P., Wakabayashi, N., Shen, Y., Zimmerman, S., Godio, L., Rodrigues-Bigas, M., Su, L.K., Sherman, J., Kelloff, G., Levin, B. and Steinbach, G. (2002) A randomised, double blind, placebo controlled study of celecoxib, a selective cyclooxygenase 2 inhibitor, on duodenal polyposis in familial adenomatous polyposis. Gut 50, 857–860.
[47] Arico, S., Pattingre, S., Bauvy, C., Gane, P., Barbat, A., Codogno, P. and Ogier-Denis, E. (2002) Celecoxib induces apoptosis by inhibiting 3-phosphoinositide-dependent protein kinase-1 activity in the human colon cancer HT-29 cell line. J. Biol. Chem. 277, 27613–27621.
[48] Elder, D.J., Halton, D.E., Playle, L.C. and Paraskeva, C. (2002) The MEK/ERK pathway mediates COX-2-selective NSAID-induced apoptosis and induced COX-2 protein expression in colorectal carcinoma cells. Int. J. Cancer 99, 323–327.
[49] Siavash, H., Nikitakis, N.G. and Sauk, J.J. (2004) Targeting of epidermal growth factor receptor by cyclopentenone prostaglandin 15-deoxy-$\Delta^{12,14}$-prostaglandin $J_2$ in human oral squamous carcinoma cells. Cancer Lett. 211, 97–103.
[50] Eucker, J., Bangeroth, K., Zavrski, I., Krebbel, H., Zang, C., Heider, U., Jakob, C., Elstner, E., Possinger, K. and Sezer, O. (2004) Ligands of peroxisome proliferator-activated receptor γ induce apoptosis in multiple myeloma. Anticancer Drugs 15, 955–960.
[51] Pang, L., Nie, M., Corbett, L. and Knox, A.J. (2003) Cyclooxygenase-2 expression by nonsteroidal anti-inflammatory drugs in human airway smooth muscle cells: role of peroxisome proliferator-activated receptors. J. Immunol. 170, 1043–1051.
[52] Munkarah, A.R., Genhai, Z., Morris, R., Baker, V.V., Deppe, G., Diamond, M.P. and Saed, G.M. (2003) Inhibition of paclitaxel-induced apoptosis by the specific COX-2 inhibitor, NS398, in epithelial ovarian cancer cells. Gynecol. Oncol. 88, 429–433.

# Transplantation of Mesenchymal Stem Cells Improves Cardiac Function in a Rat Model of Dilated Cardiomyopathy

Noritoshi Nagaya, MD; Kenji Kangawa, PhD; Takefumi Itoh, MD; Takashi Iwase, MD; Shinsuke Murakami, MD; Yoshinori Miyahara, MD; Takafumi Fujii, MD; Masaaki Uematsu, MD; Hajime Ohgushi, MD; Masakazu Yamagishi, MD; Takeshi Tokudome, MD; Hidezo Mori, MD; Kunio Miyatake, MD; Soichiro Kitamura, MD

*Background*—Pluripotent mesenchymal stem cells (MSCs) differentiate into a variety of cells, including cardiomyocytes and vascular endothelial cells. However, little information is available about the therapeutic potency of MSC transplantation in cases of dilated cardiomyopathy (DCM), an important cause of heart failure.

*Methods and Results*—We investigated whether transplanted MSCs induce myogenesis and angiogenesis and improve cardiac function in a rat model of DCM. MSCs were isolated from bone marrow aspirates of isogenic adult rats and expanded ex vivo. Cultured MSCs secreted large amounts of the angiogenic, antiapoptotic, and mitogenic factors vascular endothelial growth factor, hepatocyte growth factor, adrenomedullin, and insulin-like growth factor-1. Five weeks after immunization, MSCs or vehicle was injected into the myocardium. Some engrafted MSCs were positive for the cardiac markers desmin, cardiac troponin T, and connexin-43, whereas others formed vascular structures and were positive for von Willebrand factor or smooth muscle actin. Compared with vehicle injection, MSC transplantation significantly increased capillary density and decreased the collagen volume fraction in the myocardium, resulting in decreased left ventricular end-diastolic pressure ($11\pm1$ versus $16\pm1$ mm Hg, $P<0.05$) and increased left ventricular maximum $dP/dt$ ($6767\pm323$ versus $5138\pm280$ mm Hg/s, $P<0.05$).

*Conclusions*—MSC transplantation improved cardiac function in a rat model of DCM, possibly through induction of myogenesis and angiogenesis, as well as by inhibition of myocardial fibrosis. The beneficial effects of MSCs might be mediated not only by their differentiation into cardiomyocytes and vascular cells but also by their ability to supply large amounts of angiogenic, antiapoptotic, and mitogenic factors. (*Circulation.* **2005;112:1128-1135.**)

**Key Words:** myocytes ■ angiogenesis ■ heart failure ■ growth substances ■ transplantation

Despite advances in medical and surgical procedures, congestive heart failure remains a leading cause of cardiovascular morbidity and mortality.[1] Idiopathic dilated cardiomyopathy (DCM), a primary myocardial disease of unknown etiology characterized by a loss of cardiomyocytes and an increase in fibroblasts, is an important cause of heart failure.[2] Although myocyte mitosis and the presence of cardiac precursor cells in adult hearts have recently been reported,[3] the death of large numbers of cardiomyocytes results in the development of heart failure. Thus, restoring lost myocardium would be desirable for the treatment of DCM.

Mesenchymal stem cells (MSCs) are pluripotent, adult stem cells residing within the bone marrow microenvironment.[4] In contrast to their hematopoietic counterparts, MSCs are adherent and can be expanded in culture. MSCs can differentiate not only into osteoblasts, chondrocytes, neurons, and skeletal muscle cells but also into vascular endothelial cells[5] and cardiomyocytes.[6,7] In vitro, MSCs can be induced to differentiate into beating cardiomyocytes by 5-azacytidine treatment.[8] In vivo, MSCs directly injected into an infarcted heart have been shown to induce myocardial regeneration and improve cardiac function.[9] In addition, MSC implantation induces therapeutic angiogenesis in a rat model of hindlimb ischemia through vascular endothelial growth factor (VEGF) production by MSCs.[10,11] Myocardial blood flow abnormalities, even in the presence of angiographically normal coronary arteries, have been documented in patients with DCM.[12]

Received August 18, 2004; revision received April 28, 2005; accepted May 10, 2005.

From the Departments of Regenerative Medicine and Tissue Engineering (N.N., T.I., T.I., S.M.), Internal Medicine (N.N., M.Y., K.M.), Biochemistry (K.K., T.T.), and Cardiac Physiology (Y.M., T.F., H.M.), National Cardiovascular Center Research Institute, Osaka; the Cardiovascular Division (M.U.), Kansai Rosai Hospital, Hyogo; the Tissue Engineering Research Center (H.O.), National Institute of Advanced Industrial Science and Technology, Hyogo; and the Department of Cardiovascular Surgery (S.K.), National Cardiovascular Center, Osaka, Japan.

Reprint requests to Noritoshi Nagaya, MD, Department of Regenerative Medicine and Tissue Engineering, National Cardiovascular Center Research Institute, 5-7-1 Fujishirodai, Suita, Osaka 565-8565, Japan. E-mail nnagaya@ri.ncvc.go.jp



*Circulation* is available at http://www.circulationaha.org DOI: 10.1161/CIRCULATIONAHA.104.500447